

Appendix 7

Geochemical analysis of samples of MX-80 compacted bentonite from Block 13 / Parcel A2 of the LOT Experiment

Raúl Fernández

Urs Mäder

Margarita Koroleva

Rock-Water Interaction Group

Institute of Geological Sciences

University of Bern

NAB 08-08

Geochemical analysis of samples of MX-80 compacted bentonite from Block 13 / Parcel A2 of the LOT Experiment, Äspö Hardrock Laboratory, Sweden

September 2008

Raúl Fernández

Urs Mäder

Margarita Koroleva

Rock-Water Interaction Group

Institute of Geological Sciences

University of Bern

Keywords:

MX-80, clay, compacted bentonite, EBS, in-situ experiment,
analytical techniques, LOT Experiment, Äspö

Table of Contents

Table of Contents	I	
List of Tables.....	III	
List of Figures	IV	
1	Introduction and objectives	1
2	Sample material	3
2.1	LOT parcel A2 and Block 13.....	3
2.2	Recovery of Block 13	5
2.3	Generic information on bentonite used for LOT	9
3	Physico-chemical conditions during the LOT experiment.....	11
4	Analytical program, methods, sample preparation	17
4.1	Analytical program	17
4.2	Analytical methods	17
4.2.1	Water content.....	17
4.2.2	XRD analysis	17
4.2.3	Wet and dry density	18
4.2.4	Aqueous leachates	18
4.2.5	Exchangeable cations.....	19
4.2.6	Sum of measured exchangeable cations	19
4.2.7	Cation exchange capacity by Na-acetate / Mg-nitrate displacement	19
4.2.8	Analysis of total carbon and sulfur	20
4.3	Sample preparation	20
4.3.1	Sample preparation at the Äspö URL	21
4.3.2	XRD analysis	23
4.3.3	Wet and dry density	25
4.3.4	Aqueous leachates	25
4.3.5	Exchangeable cations.....	25
4.3.6	Cation exchange capacity by Na-acetate / Mg-nitrate displacement	25
4.3.7	Total carbon and sulfur	25
5	Results.....	27
5.1	Water content.....	27
5.2	XRD analysis	28
5.3	Wet and dry density	29
5.4	Aqueous leachates	30
5.5	Exchangeable cations.....	31
5.6	Sum of measured exchangeable cations	33
5.7	Cation exchange capacity determined by Na/Mg displacement	33

5.8 Total carbon and sulfur 34

6 Comments and discussion 37

6.1 Water content..... 37

6.2 XRD analysis 37

6.3 Wet and dry density 37

6.4 Aqueous leachates 38

6.5 Exchangeable cations and sum of cations..... 38

6.6 Cation exchange capacity by Na/Mg displacement 39

6.7 Carbon and sulfur 39

6.7 Additional issues..... 41

6.8 Recommendations 41

Acknowledgments..... 43

References 45

Appendix A - Water content data A-1

Appendix B - XRD data B-7

Appendix C - Aqueous extract data..... C-21

Appendix D - Exchangeable cation data D-23

List of Tables

Table 1:	Mineralogical composition of the Wyoming bentonite material used for fabricating the bentonite blocks. (data from O. Karnland, Clay Technology).....	9
Table 2:	Water ratio of bentonite material from different positions in parcel A2 relative to dry mass. Position indicates radial distance [cm] from Cu-tube (data from O. Karnland, Clay Technology).....	13
Table 3:	Density of bentonite material from different positions in parcel A2. Position indicates radial distance [cm] from Cu-tube. All data values in kg/m ³ (data from O. Karnland, Clay Technology).....	14
Table 4:	Degree of saturation of bentonite material from different positions in parcel A2. Position indicates radial distance [cm] from Cu-tube (data from O. Karnland, Clay Technology)	15
Table 5:	Sample labels and radial width of the subsamples of the N and S profiles	23
Table 6:	Sample labels and radial width of the subsamples of the West profile	23
Table 7:	Water content relative to 105 °C and radial width of the subsamples of the N and S profiles	27
Table 8:	Measured water content in samples W-3 and W-4 relative to 105 °C (/1 and / 2 denote duplicates).....	28
Table 9:	Measured XRD samples	29
Table 10:	Measured Bulk Densities.....	30
Table 11:	Corrected distribution of exchangeable cations (meq/100 g dry mass).....	32
Table 12:	Cation exchange capacity and calcium dissolved from calcite (meq/100 g).....	34
Table 13:	Total, inorganic and organic carbon and total sulfur on the West profile samples	35
Table 14:	Averaged values of duplicates of the West profile: aqueous and exchangeable calcium, inorganic and aqueous carbon (as CO ₃ ²⁻), total and aqueous sulfur (as SO ₄ ²⁻) and aqueous chloride. All values relate to 100 g of dry sample.....	40
Table 15:	Water content as a function of temperature and distance from the copper heater in the North profile (Lower and Upper).....	1
Table 16:	Water content as a function of temperature and distance from the copper heater in the South profile (Lower and Upper).....	1
Table 17:	Aqueous extract concentrations in samples from LOT A2, Block 13 (mmol/l).....	22
Table 18:	Uncorrected concentrations of exchangeable cations recalculated to dry mass (meq/100 g) and total Ni consumption	23

List of Figures

Figure 1:	Layout of the LOT parcel A2. Blocks equipped with sensors or test materials are numbered, from bottom to top. Block 13 (barren, not numbered) is located at a depth of 2.7 m (scale on left) (figure from O. Karnland, Clay Technology).....	4
Figure 2:	Sample orientation and labeling scheme used in the LOT series of experiments. SE and NW denote the directions of compass in the test-hole, figures denote the radial position of the centre of the specimens expressed in centimetres measured from the block inner mantel surface (interface to heater), and A, B and C denote the analysed three vertical positions in the blocks (figure from O. Karnland, Clay Technology).....	5
Figure 3:	LOT parcel A2 ready to be lifted. The stack of bentonite blocks is completely contained in an outer rind of granite (image from O. Karnland, Clay Technology)	6
Figure 4:	The lower part of the LOT parcel A2. The diameter of the bentonite blocks is 30 cm, stacked on the central copper tube. Sensor wires are located along the outside of the bentonite blocks (peeled back before dissection). The deep end is still contained within a rind of granite	6
Figure 5:	Protection of the bentonite section from drying out between the 1 st and 2 nd day of sampling	7
Figure 6:	Block 13 secured with a supporting nylon strap, and marked for cutting. The thickness of a block is 10 cm, the outer diameter 30 cm, and the inner diameter 11 cm. The radial width is 9.5 cm.....	7
Figure 7:	The removal of the “doughnut” block 13	8
Figure 8:	Martin Birgersson from Clay Technology with the successfully removed block 13. The groove marks the top of the block and the North orientation. North is also marked by a red pin placed on the side of the block	8
Figure 9:	Composition of Na-montmorillonite of the Wyoming bentonite reference material indicated as a triangle in the Beidellite (B) – Montmorillonite (M) range. The basis is $O_{20}(OH)_4$ (Karnland and Birgersson 2006, modified from Newman and Brown, 1987).....	10
Figure 10:	Vertical section displaying the radial stable temperature distribution. Temperatures are constrained at the level of block 14, just 10 cm above block 13. It can be inferred that block 13 was exposed to temperatures of 130 - 140 °C at the interface to the central copper tube (data and graph from O. Karnland, Clay Technology)	11
Figure 11:	Temperature distributions in block no 14. The denomination A2141T indicates the temperature 1 cm from the central copper tube (in parcel A2, block 14), and A2148T indicates the temperature 8 cm from the copper tube, which is 1 - 2 cm from the rock (data and graph from O. Karnland, Clay Technology).....	12
Figure 12:	Sample block 13 (LA2-13) wrapped in plastic foil marked and ready for cutting. The top surface is oriented up in the experiment, and the radial orientation is relative to North. Two radial slabs were first cut, labelled N and S	21

Figure 13:	Cutting block 13 with a brand new band-saw in one of the surface laboratories at Äspö.....	22
Figure 14:	Two slabs marked for cutting 4 radial profiles for the measurement of water content. The profiles are labelled NU (North, upper profile), NL (North, lower profile), SU (South, upper profile), and SL (South, lower profile). The lines marking the cuts for the segments are only approximate.....	22
Figure 15:	Western half of block 13 (LOT parcel A2) used to cut a vertical profile oriented towards the West (tip of pen).....	24
Figure 16:	Cut profile from block 13. The heater was in contact along the right side (curved surface), and the contact to granite was along the left side. The lower edge represents the base of block 13.....	24
Figure 17:	Cut profile from block 13 after subsampling. The larger pieces were processed to perform the CEC, ion selectivity and XRD analyses. Some reference samples were kept sealed and refrigerated (for water content, density).....	25
Figure 18:	Aqueous species distribution in the aqueous leachates as function of their proximity to the copper heater (meq/100 g dry mass).....	31
Figure 19:	Distribution of exchangeable cations as a function of sample position relative to the copper heater for case I (Na corrected for aqueous Cl equivalents and Ca for aqueous SO ₄) and case II (Na corrected for aqueous Cl + SO ₄ equivalents).....	32
Figure 20:	Sum of measured exchangeable cations as function to the sample position relative to the copper heater applying corrections (cases I and II) as described above.....	33
Figure 21:	Comparison between the sum of measured exchangeable cations by the Ni(en) method (average of duplicate analyses) and the cation exchange capacity measured by the Na/Mg displacement method related to the sample position from the copper heater.....	34
Figure 22:	Inorganic and aqueous carbon (soluble as CO ₃ ²⁻) and total and aqueous sulfur (soluble as SO ₄ ²⁻) distribution related to the sample position from the copper heater.....	41
Figure 23:	Water content in the North-Lower profile as a function of time of drying and drying temperature augmented incrementally.....	2
Figure 24:	Water content in the North-Upper profile as a function of time of drying and drying temperature augmented incrementally.....	2
Figure 25:	Water content in the South-Lower profile as a function of time of drying and drying temperature augmented incrementally.....	3
Figure 26:	Water content in the South-Upper profile as a function of time of drying and drying temperature augmented incrementally.....	3
Figure 27:	Water content at selected temperatures in the North-Lower profile in function of the distance from the heater.....	4
Figure 28:	Water content at selected temperatures in the North-Upper profile in function of the distance from the heater.....	4

Figure 29:	Water content at selected temperatures in the South-Lower profile in function of the distance from the heater	5
Figure 30:	Water content at selected temperatures in the South-Upper profile in function of the distance from the heater	5
Figure 31:	Comparison of the water content in all profiles at 105 °C, in function of the distance from the heater	6
Figure 32:	Disoriented bulk samples: Profile W1 to W4 compared to reference sample (REF-Bulk). Cr = cristobalite; Q = quartz	8
Figure 33:	Test samples for optimizing measurement conditions. Cr = cristobalite; Q = quartz; Fel = feldspars; M = montmorillonite.....	9
Figure 34:	Oriented clay samples, 18 hours of sedimentation. Profile W1 to W4 compared to reference. Cr = cristobalite; Q = quartz; M = montmorillonite; Sap = saponite.....	10
Figure 35:	Oriented clay samples, 72 hours of sedimentation. Profile W1 to W4 compared to reference. See Figure 34 for peak labels.....	11
Figure 36:	Comparison between 18 and 72 hours of sedimentation, reference sample. See Figure 34 for peak labels.....	12
Figure 37:	Comparison between 18 and 72 hours of sedimentation, profile sample W4 (cold end). See Figure 34 for peak labels	13
Figure 38:	Comparison between 18 and 72 hours of sedimentation, profile sample W3. See Figure 34 for peak labels.....	14
Figure 39:	Comparison between 18 and 72 hours of sedimentation, profile sample W2. See Figure 34 for peak labels.....	15
Figure 40:	Comparison between 18 and 72 hours of sedimentation, profile sample W1 (hot end). See Figure 34 for peak labels	16
Figure 41:	Profile sample W4 (cold end): x = dry sample; y = ethylenglicol saturated; z = heated at 550 °C for 2 h	17
Figure 42:	Profile sample W3: x = dry sample; y = ethylenglicol saturated; z = heated at 550 °C for 2 h.....	18
Figure 43:	Profile sample W2: x = dry sample; y = ethylenglicol saturated; z = heated at 550 °C for 2 h.....	19
Figure 44:	Profile sample W2, W3 and W4 (cold end): oriented dry samples	20

1 Introduction and objectives

The Rock-Water Interaction Group of the Institute of Geological Sciences at the University of Bern was contracted by Nagra to perform analytical work for bentonite samples from the LOT experiment (Äspö Hardrock Laboratory) within the framework of a Nagra-SKB cooperation.

The aim of this work is to apply the analytical techniques tested and developed for the analysis of claystone (Opalinus Clay from Mont Terri and the Zürcher Weinland area, Switzerland; Callovo-Oxfordian claystone from the Bure area, France), and compare them with the techniques and procedures employed by Clay Technology AB that is performing most of the analytical work for the various parcels of the LOT experiment. This effort is expected to broaden the data basis and strengthen its interpretation. The resolution of any inconsistencies will help to optimize analytical techniques, and better assess their relative merits.

This report emphasises the results of the analytical work and methods used, and offers limited interpretation. The report is intended as a basis for discussion regarding the in-depth interpretation and the assessment of the relative merits of alternate analytical techniques.

The objectives of SKB in the LOT test series are to validate models and hypotheses concerning long term processes in the bentonite buffer material and of related processes regarding microbiology, radionuclide transport and copper corrosion under conditions similar to those expected in a KBS-3 repository design foreseen by SKB for deep disposal of high-level radioactive waste.

The Parcel A2 of the LOT Experiment was excavated in January 2006. The analytical work reported here was performed during 2006, and a draft data report was issued in January 2007. The report was completed, reviewed and revised during 2007. Results were presented at the LOT Project Meetings in Äspö (Nov. 2006) and Lund (Nov. 2007).

2 Sample material

The LOT experiment, carried out at the Äspö Hardrock Laboratory in Sweden, consists of seven parcels emplaced in large-diameter vertical boreholes in granite, each one consisting of a central heater surrounded by a stack of compacted bentonite blocks (doughnuts). The stack is instrumented for monitoring physical conditions during the experiment, and contains a variety of special-purpose doughnuts designed for specific tasks such as corrosion studies, or for obtaining geochemical information. The parcels are left in place for a desired length of time (years) and are then excavated, dissected and prepared for analysis (see below).

2.1 LOT parcel A2 and Block 13

The layout of the LOT parcel A2 is shown in Figure 1. The parcel was emplaced at the end of October, 1999, and the heater was turned on February 2, 2000. The heater was turned off December 5, 2005, and the parcel was excavated between January 9 and 16, 2006. The duration of the experiment was therefore approximately 6 years, whereby a steady-state heat flow condition was reached after the 1st year. The experimental site was located in the G-tunnel at the -450 m level of the Äspö Laboratory.

Block 13 (sample label LA2-13) is located at a depth of approximately 2.7 m (Figure 1) measured from the floor of the gallery and is contained within the hottest zone of the experiment (see below). The underlying block, No 12, contains 10 % anhydrite (CaSO_4) as discrete embedded plugs as well as a sampling cup for porewater (if present). The overlying block, No 14, is barren, except for 6 temperature sensors and several pressure sensors (contacting materials are Ti and CuNi alloy).

The central heater is contained in a heavy-walled copper tube (11 cm outer diameter), and the diameter of the borehole is 30 cm. The bentonite blocks were only slightly undersized to fit into the borehole snugly, and they have a radial width after swelling of 9.5 cm, and a height of 10 cm.

Initially, an annular gap of approximately 10 mm existed between the bentonite blocks and the borehole wall in the granite (partially occupied by Ti and CuNi tubing containing the sensor connections). This gap was filled with formation water after sealing of the parcel and before the heater was turned on. This water was intended to induce rapid initial swelling of the outermost part of the bentonite blocks in order to close the gap. It can also be assumed that the small annular gap between the copper heater and the bentonite doughnuts was wetted as well when the outer free volume was filled with formation water. It may therefore be assumed that the contact between the heater and the bentonite as well as that between the bentonite and the granite was already tight when the heater was turned on 3 months after installation.

The standard analytical program set up by Clay Technology (not including this study) includes the following, with methods indicated in parentheses:

- water ratio (oven drying)
- density (weighing in paraffin oil)
- hydraulic conductivity (oedometer)
- swelling pressure (oedometer)
- swelling capacity (free swelling in test tube)
- shear strength (uniaxial compression tests, triaxial tests)
- element concentration in porewater (chemical analysis)

- element content in the bulk and clay fraction material (ICP-AEM)
- cation exchange capacity (Cu- trien)
- distribution of exchangeable ions (ammonium exchange)
- mineralogical composition of bulk and clay fraction (XRD, SEM-EDX)
- microstructure (TEM and SEM-EDX)

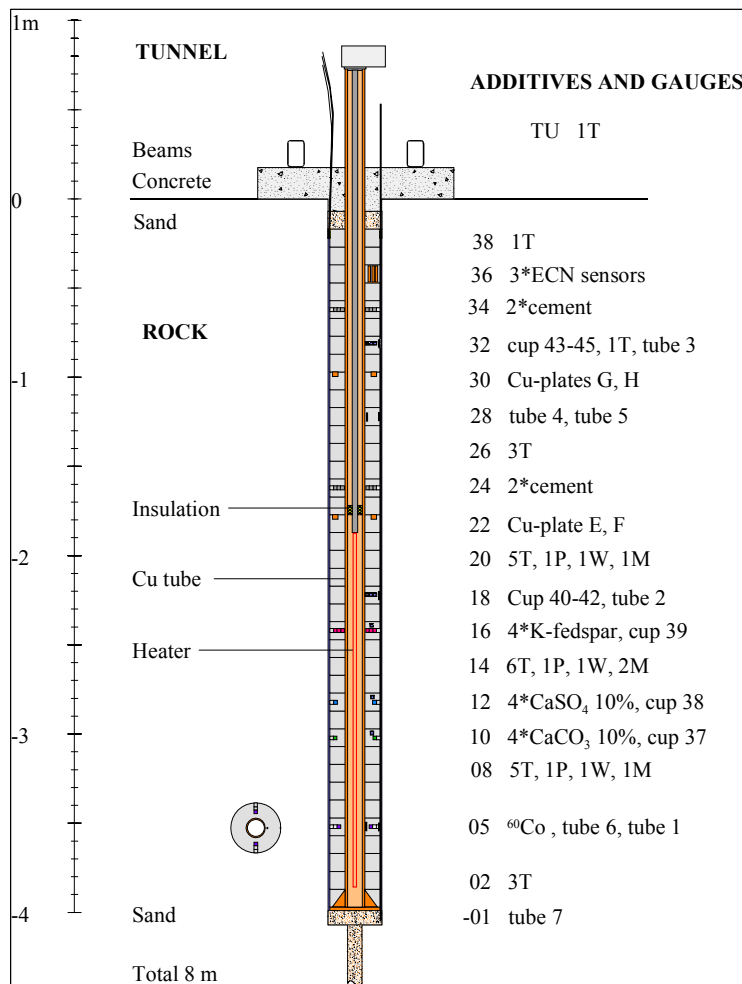


Figure 1: Layout of the LOT parcel A2. Blocks equipped with sensors or test materials are numbered, from bottom to top. Block 13 (barren, not numbered) is located at a depth of 2.7 m (scale on left) (figure from O. Karnland, Clay Technology)

The sample orientation scheme for the LOT experiment was also used in this study, and sample numbers according to this scheme are also provided in addition to our internal sample numbers. Figure 2 illustrates the sample orientation and labelling scheme.

An example illustrates the method: 08ASE3 where

- 08 block number (counted from the bottom of the parcel)
- A vertical level in the block (A or B or C)
- SE direction of compass in the test hole
- 3 radial distance in centimeters from the inner mantel surface to the center of the specimen.

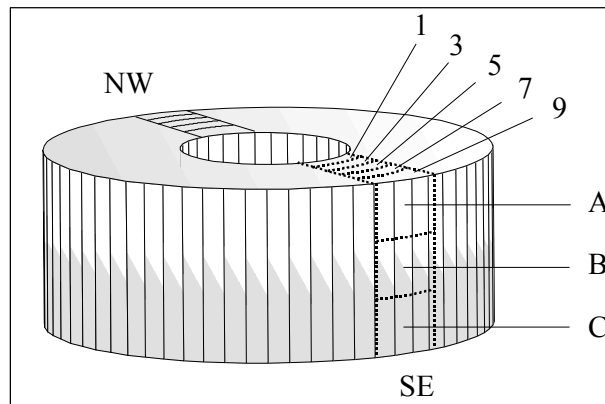


Figure 2: Sample orientation and labeling scheme used in the LOT series of experiments. SE and NW denote the directions of compass in the test-hole, figures denote the radial position of the centre of the specimens expressed in centimetres measured from the block inner mantel surface (interface to heater), and A, B and C denote the analysed three vertical positions in the blocks (figure from O. Karnland, Clay Technology)

2.2 Recovery of Block 13

The LOT parcel A2 was extracted as a cylindrical block preserving a rind of granite (Figures 3 and 4). The excavated cylinder was dissected near the experimental location by first gradually removing the enclosing granite, followed by separating the bentonite blocks. Drying out was minimized by covering the parcel in between working episodes (Figure 5), by wrapping samples immediately after removal from the central heater tube, and also by the relatively high ambient humidity.



Figure 3: LOT parcel A2 ready to be lifted. The stack of bentonite blocks is completely contained in an outer rind of granite (image from O. Karland, Clay Technology)



Figure 4: The lower part of the LOT parcel A2. The diameter of the bentonite blocks is 30 cm, stacked on the central copper tube. Sensor wires are located along the outside of the bentonite blocks (peeled back before dissection). The deep end is still contained within a rind of granite



Figure 5: Protection of the bentonite section from drying out between the 1st and 2nd day of sampling

Block 13 was removed in the same way as all other blocks, by measuring the thickness of 10 cm, and cutting the block with a power saw to very close to the copper tube (Figure 6). The block could then be pried loose and slid off the central tube in a single piece (Figures 7 and 8). The block was tightly wrapped for short interim storage before it was carried to the surface to be further processed in one of the laboratory rooms at the Äspö Laboratory surface facilities.



Figure 6: Block 13 secured with a supporting nylon strap, and marked for cutting. The thickness of a block is 10 cm, the outer diameter 30 cm, and the inner diameter 11 cm. The radial width is 9.5 cm



Figure 7: The removal of the “doughnut” block 13



Figure 8: Martin Birgersson from Clay Technology with the successfully removed block 13. The groove marks the top of the block and the North orientation. North is also marked by a red pin placed on the side of the block

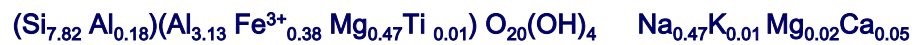
2.3 Generic information on bentonite used for LOT

Na-exchanged Wyoming bentonite (MX-80) was used for fabricating the bentonite blocks for all of the LOT parcels. Table 1 is a summary of mineralogy (data from O. Karnland, presented at a LOT meeting 2006) as determined by X-ray diffraction analysis.

Table 1: Mineralogical composition of the Wyoming bentonite material used for fabricating the bentonite blocks. (data from O. Karnland, Clay Technology)

Minerals %	MX-80
Albite	7
Cristobalite	3
Gypsum	1
Muscovite	1
Quartz	5
Na-Montmorillonite	83
	100

The chemical formula of the Na-montmorillonite of the reference material is (O. Karnland, Clay Technology):



The composition is indicated in Figure 9 within the nomenclature adopted by Clay Technology (Karnland and Birgersson 2006).

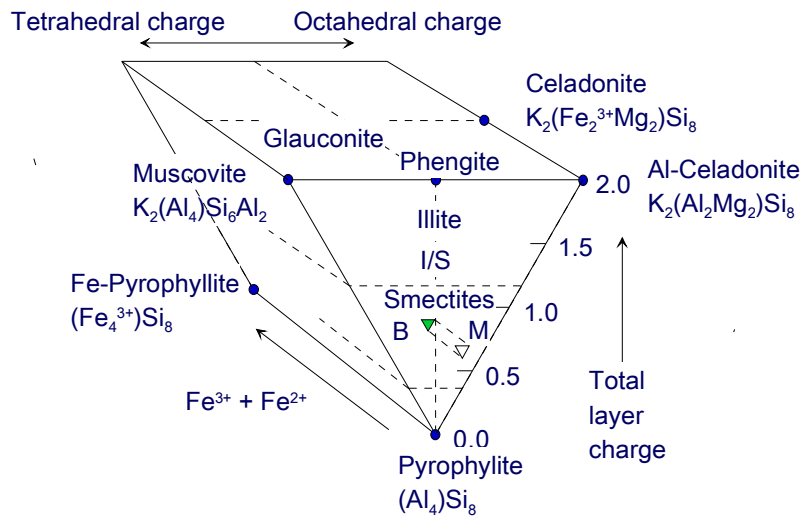


Figure 9: Composition of Na-montmorillonite of the Wyoming bentonite reference material indicated as a triangle in the Beidellite (B) – Montmorillonite (M) range. The basis is $O_{20}(OH)_4$ (Karlund and Birgersson 2006, modified from Newman and Brown, 1987)

3 Physico-chemical conditions during the LOT experiment

Parcel A2 of the LOT experiment reached stable temperature conditions after 1 year, and remained at constant temperature for an additional 5 years. The overall temperature distribution in the LOT parcel A2 is synthesized in Figure 10. The temperature distribution in block 14 (just 10 cm above block 13) is shown in Figure 11. Block 13 was therefore subject to temperatures of $\sim 135\text{ }^{\circ}\text{C}$ at the contact to the heater, and $\sim 85\text{ }^{\circ}\text{C}$ at the contact to the granite.

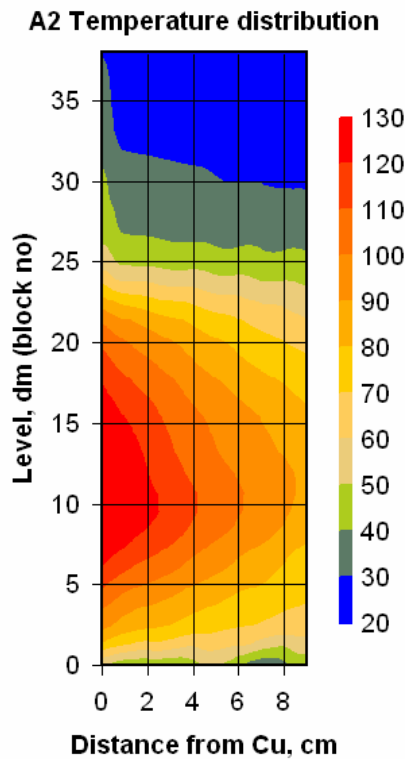


Figure 10: Vertical section displaying the radial stable temperature distribution. Temperatures are constrained at the level of block 14, just 10 cm above block 13. It can be inferred that block 13 was exposed to temperatures of $130 - 140\text{ }^{\circ}\text{C}$ at the interface to the central copper tube (data and graph from O. Karnland, Clay Technology)

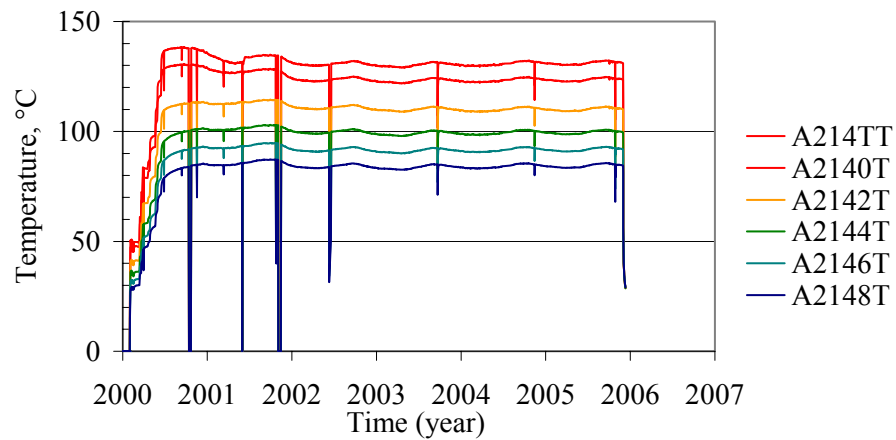


Figure 11: Temperature distributions in block no 14. The denomination A2141T indicates the temperature 1 cm from the central copper tube (in parcel A2, block 14), and A2148T indicates the temperature 8 cm from the copper tube, which is 1 - 2 cm from the rock (data and graph from O. Karland, Clay Technology)

The heater was turned off on December 5, 2005, and left to cool until excavation started on January 9 and ended on January 16, 2006. There was therefore a 4 - 5 week period during which temperatures were decreasing, and some chemico-physical re-adjustments may have occurred.

Preliminary data from Clay Technology on water content (Table 2), density (Table 3) and degree of saturation (Table 4) are shown below for reference.

Table 2: Water ratio of bentonite material from different positions in parcel A2 relative to dry mass. Position indicates radial distance [cm] from Cu-tube (data from O. Karnland, Clay Technology)

Position	1	3	5	7	9
Block no					
38	0.376	0.380	0.374	0.393	0.408
33	0.321	0.321	0.320	0.325	0.337
31	0.309	0.305	0.309	0.316	0.336
29	0.301	0.299	0.304	0.314	0.331
27	0.309	0.303	0.304	0.312	0.333
25	0.299	0.301	0.304	0.320	0.340
23	0.293	0.293	0.299	0.313	0.332
21	0.285	0.289	0.293	0.304	0.326
19	0.287	0.285	0.303	0.317	0.333
17	0.282	0.278	0.295	0.308	0.324
15	0.280	0.279	0.300	0.316	0.330
11	0.268	0.271	0.279	0.297	0.316
9	0.269	0.271	0.282	0.303	0.318
7	0.275	0.274	0.283	0.298	0.314

Table 3: Density of bentonite material from different positions in parcel A2. Position indicates radial distance [cm] from Cu-tube. All data values in kg/m^3 (data from O. Karnland, Clay Technology)

Position	1	3	5	7	9
Block no					
38	1864	1876	1859	1862	1847
33	1923	1922	1920	1918	1897
31	1941	1948	1943	1930	1898
29	1955	1962	1954	1941	1912
27	1954	1962	1957	1945	1912
25	1965	1960	1953	1916	1890
23	1977	1971	1964	1943	1917
21	1982	1978	1969	1955	1928
19	1979	1981	1962	1940	1921
17	1983	1987	1948	1951	1928
15	1977	1985	1959	1942	1919
11	1987	1993	1979	1950	1933
9	1990	1988	1975	1951	1934
7	2000	1991	1975	1954	1936

Table 4: Degree of saturation of bentonite material from different positions in parcel A2. Position indicates radial distance [cm] from Cu-tube (data from O. Karland, Clay Technology)

Position	1	3	5	7	9
Block no					
38	1.007	1.024	0.998	1.024	1.026
33	0.995	0.993	0.990	0.995	0.991
31	0.996	0.998	0.998	0.994	0.990
29	0.999	1.004	1.003	1.004	0.998
27	1.011	1.010	1.006	1.005	1.000
25	1.006	1.004	1.002	0.985	0.987
23	1.011	1.004	1.005	1.004	1.004
21	1.003	1.006	1.001	1.005	1.007
19	1.004	1.001	1.010	1.008	1.011
17	1.000	0.997	0.982	1.005	1.005
15	0.988	0.995	1.002	1.008	1.004
11	0.979	0.990	0.989	0.986	0.998
9	0.984	0.986	0.990	0.998	1.003
7	1.007	0.993	0.993	0.993	0.998

The bentonite may be assumed to be fully saturated in the entire parcel, including the hottest zone. The tendency towards saturation values slightly below 1.00 observed in the hottest zone (Table 4) may reflect the effect of thermal contraction after cooling. It should be noted that there is a strong correlation between water content and density, and thus full saturation does not imply a uniform water content.

4 Analytical program, methods, sample preparation

4.1 Analytical program

The analytical program for the analysis at the University of Bern included the following parameters. The aim was not to perform a complete or most optimal analytical program, but to apply those methods that were used previously for the analysis of claystones, and thus allow for some comparison with the analytical program of Clay Technology.

- Measurement of water content
- XRD on bulk samples and grain size fractions
- Wet and dry density measured in paraffin oil on select samples
- Cations and anions on aqueous leachates
- Exchangeable cations using the Ni-ethylenediamine method corrected for disturbing effects
- Sum of measured exchangeable cations
- Cation exchange capacity by Na-acetate / Mg-nitrate displacement
- Content of C(inorganic), C(total), and S(total) in select samples

4.2 Analytical methods

4.2.1 Water content

Water content was measured by heating the clay samples in a drying oven. All samples were placed in plastic containers and dried at 40 °C for 20 days. After this period the samples were changed to glass dishes and the temperature increased to 70 °C, maintaining this temperature for 5 days to reach constant mass. This was repeated to higher temperatures, and drying times were: 1 day at 90 °C, 6 days at 105 °C, and 19 days at 150 °C.

The water content was calculated relative to the dry mass obtained at 105 °C by the following equation:

$$\text{Water content (\%)} = \frac{m_{\text{initial}} - m_{105^{\circ}\text{C}}}{m_{105^{\circ}\text{C}}} \times 100$$

The mass of the samples was weighed periodically, recording all mass losses. The water loss as a function of temperature was also evaluated, whereby the measurements were extended to constant mass at each temperature.

4.2.2 XRD analysis

Mineralogical analyses of the bulk sample and different clay fractions were made by X-ray diffraction analysis on disoriented and oriented rock powders using a PHILIPS PW-3710 diffractometer. The system uses $\text{Cu}_{K\alpha}$ radiation with a wavelength of 1.54Å. Current intensity and voltage were 30 mA and 40 kV, respectively.

Total bulk samples and clay fraction samples were determined by scanning from 2 to 70° and from 2 to 40° 2θ, respectively, with 0.02° step size and 1 second counting time per step.

4.2.3 Wet and dry density

Bulk wet density ($\rho_{b,wet}$) was measured in duplicate using the paraffin oil displacement method. The principle of the method is the calculation of bulk wet density from the sample mass and its volume. The volume was determined by weighing a sample first in air, and then weighing it while immersing the sample in paraffin oil ($\rho_p = 0.86 \text{ g/cm}^3$ at 20 °C), making use of Archimedes' principle. The mass of a beaker filled with paraffin oil was measured before (m_p) and after (m_{p+r}) immersion of the sample, which was let hang freely on a thin thread fixed to a tripod. The bulk wet density was calculated according to:

$$\rho_{b,wet} = \frac{\rho_p \times m_{rock+pw}}{m_{p+r} - m_p}$$

where $m_{rock+pw}$ is the mass of the wet rock sample, m_p is the mass of the beaker with paraffin oil and m_{p+r} is the measured mass of the beaker with paraffin oil and the immersed freely hanging sample.

Two separate homogeneous and physically intact samples of 2 - 3 cm³ volume were measured.

Bulk dry density ($\rho_{b,dry}$) was calculated from the water content and the bulk wet density according to:

$$\rho_{bdry} = \frac{\rho_{b,wet}}{1 + 0.01 \times WC}$$

where WC is the water content value (%).

4.2.4 Aqueous leachates

6 g of dried bentonite was added to 60 ml of distilled water (S:L ratio 1:10) and shaken end-over-end for two days. The mix was centrifuged two times for 1 hour, and the supernatant solution filtered with a 0.2 µm filter. Additional centrifuging yielded approximately one more milliliter of solution that was not used, however, for analysis. Sample W-4B was centrifuged three times before filtration to increase the initially low yield.

Alkalinity (by titration) and pH were determined immediately after termination of the extraction procedure. Major cations (Na^+ , K^+ , Ca^{2+} and Mg^{2+}) and anions (F^- , Cl^- , Br^- , SO_4^{2-} and NO_3^-) were determined using a Metrohm 861 Compact Ion Chromatograph with a relative error of $< \pm 5 \%$. Sr^{2+} was measured by Atomic Absorption Spectroscopy (AAS) in a Varian SpectrAA 300 instrument because its concentrations were below the detection limit for ion chromatography.

4.2.5 Exchangeable cations

Samples were mixed with 30.0 ml of a nickel ethylenediamine (Ni-en) 0.5 M solution using a S:L ratio of 0.5:1. All samples were shaken end-over-end for 2 days in polypropylene tubes. After phase separation by centrifuging (1 hour at 5200 rpm), the supernatant leachate was removed using a syringe and filtered to $< 0.2 \mu\text{m}$.

The exchangeable cation population was displaced with Ni(en) as proposed by Bradbury and Baeyens (1998). The method takes advantage of the high selectivity of the Ni(en) complex which displaces all exchangeable cations from the clay minerals into solution. The pH of the Ni(en) solution is buffered to 8.1 - 8.2 by adding HNO₃ Titrisol™ solution which is equivalent to the pH of a calcite saturated solution at a P_{CO_2} of $10^{-3.5}$ bar and consequently a solution in equilibrium with air. Then, the solution is filtered and analyzed.

Analyses of major cations (Na⁺, K⁺, Ca²⁺, Mg²⁺ and Sr²⁺) and nickel were performed by AAS. The Cumulative error of the measurements is approximately $\pm 5 \%$.

The obtained Ca²⁺ and Na⁺ exchangeable cation concentrations should be corrected for the contributions from the porewater or any soluble salts with the chloride and sulfate concentrations measured in the aqueous leachates to obtain “true” amounts on the exchanger (see results and discussion).

4.2.6 Sum of measured exchangeable cations

It has been assumed that some calcium and sodium measured as exchangeable cations by AAS actually originate from the dissolution of NaCl and CaSO₄ soluble salts contained in the dried sample. This has been corrected by combining all chloride with sodium and all sulfate with calcium, and considering the remaining concentrations as exchangeable. No correction has been performed to potassium, magnesium or strontium. This issue – and some alternative assumptions – are discussed below.

Thus, the sum of exchangeable cations is taken as the sum of extracted K⁺, Mg²⁺ and Sr²⁺ plus the sum of remaining Na⁺ and Ca²⁺ after corrections.

4.2.7 Cation exchange capacity by Na-acetate / Mg-nitrate displacement

The method used is a modification of the one proposed by Rhoades (1982) developed for soils. It was refined and used for bentonite at the University Autónoma de Madrid within the Geochemistry of Clays research group.

0.25 g of dry sample were weighed and placed in a centrifuge tube, and 20 ml of sodium-acetate buffer solution were added (AcONa, 1M, pH = 8.2). This was done on duplicate samples. The mixture was let reacting for 24 hours in an end-over-end shaker. During this period Na⁺ saturates the exchangeable cation positions while displacing the original cation population to the solution. The selected pH in solution is supposed to minimize the dissolution of any accessory minerals, calcite in particular, or salt precipitates formed during drying of the sample.

After this, the tube was ultrasonically agitated for 5 minutes and stirred for 30 minutes in an orbital stirrer. Then, the tube was centrifuged for 10 minutes at 4500 rpm. Right afterwards, the solution was decanted and discarded, and the solid sample was washed two more times with 20 ml of AcONa 1M, again including ultrasonic and orbital agitation and centrifuging.

Then, the sample was washed with 20 ml of ethanol to remove the excess of salts, again 3 times, following the method described above with ultrasonic and orbital stirring steps and centrifuging. For the third time, just 10 ml of ethanol were added.

Finally, sodium was displaced from the exchangeable positions by saturation with magnesium by washing with a $Mg(NO_3)_2$ 1M solution (pH ~ 5). 15 ml of magnesium nitrate solution were added to the remaining solid sample, following again the same method for three times (5 minutes of ultrasonic agitation, 30 minutes in the orbital stirrer, and 5 minutes of centrifugation) but now collecting all the solution in a 50 ml flask.

The flask with the collected solutions was filled to the 50 ml level with distilled water. The solid sample can be discarded.

Finally, Na^+ was measured by AAS and the CEC calculated as:

$$CEC(meq/100g) = \frac{Na^+(mmoles)}{m_{dry}} \times 5$$

A small density correction was applied in order to account for the density of the Mg-nitrate solution, depending on the concentration units used.

4.2.8 Analysis of total carbon and sulfur

Between 50 and 100 mg of dried sample (at 105 °C) was used to measure total and inorganic carbon and total sulfur in the West profile.

Total sulfur and total carbon were determined by coulometry in a CS-MAT-5500 carbon and sulfur analyzer (Ströhlein Instruments). The principle of the method is based on the oxidation of carbon and sulfur species to CO_2 and SO_2 by applying oxidative atmosphere at high temperature (1350 - 1550 °C). The solid sample for analysis is combusted in a high frequency furnace in a ceramic crucible in an oxygen stream. The reaction gases CO_2 and SO_2 produced during combustion are quantified by Non-Dispersive Infrared (NDIR) spectroscopy, giving the results of total carbon and sulfur. Inorganic carbon is determined by acidification. Organic carbon was obtained by subtracting inorganic carbon from the total carbon.

The detection limit for S is approximately 0.1 wt%, and that for C likely better than 0.5 wt%, a quantity established for carbon-rich samples. The detection of organic carbon in carbon-poor materials such as bentonite is therefore difficult if not impossible by this method.

4.3 Sample preparation

All sample preparation and handling (crushing, leaching, etc.) of air-dried rock material was performed under ambient laboratory conditions. Two North to South profiles (30 samples in total) were cut to measure the water content, and these samples were prepared on-site at Äspö a short time after the recovery of Block 13. A profile extending towards the West (4 samples) was cut for all other analytical measurements, and these samples were prepared at the University of Bern.

4.3.1 Sample preparation at the Äspö URL

Four sample profiles were prepared on site at Äspö for water content measurements. Two profiles extend to the North, and two profiles to the South, whereby one of each profiles represents the lower half of the doughnut (relative to its position in the borehole), and the other one the upper half (Figure 12).

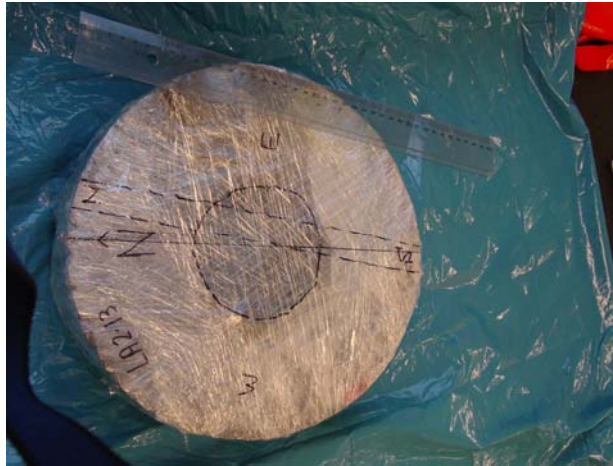


Figure 12: Sample block 13 (LA2-13) wrapped in plastic foil marked and ready for cutting. The top surface is oriented up in the experiment, and the radial orientation is relative to North. Two radial slabs were first cut, labelled N and S

The bentonite block was cut with an electric band-saw (Figure 13). The radial sections were further cut into an upper and lower half, and segmented into 7 and 8 subsamples, respectively (Figure 14). The marks on the plastic wrapping shown in Figure 14 are only schematic and do not represent the cutting as carried out.

All samples were immediately weighed after cutting and enclosed in vials. The vials were packed under a slight vacuum for transport, and brought to Bern by Urs Mäder by air plane. The two large off-cuts of block 13 were also vacuum-packed and transported to Bern for further analysis. The vacuum packaging technique allows for easy inspection of the tightness of the seal simply by the state of preservation of the vacuum. The vacuum need not be strong (avoid evaporation) and corresponds to that achieved by a commercial household vacuum sealing device used for general food wrapping and preservation.

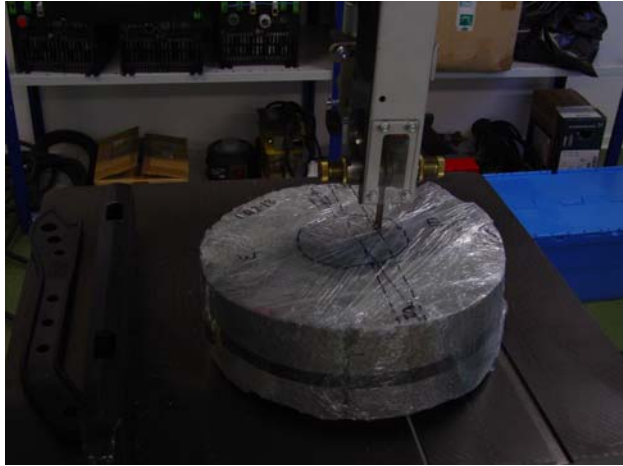


Figure 13: Cutting block 13 with a brand new band-saw in one of the surface laboratories at Äspö



Figure 14: Two slabs marked for cutting 4 radial profiles for the measurement of water content. The profiles are labelled NU (North, upper profile), NL (North, lower profile), SU (South, upper profile), and SL (South, lower profile). The lines marking the cuts for the segments are only approximate

The radial width of the samples used for the water content analysis is given in Table 5, including 8 segments for the North profile and 7 segments for the South profile. The mass of the samples varies between 11 and 60 g depending on radial width, all having approximately the same thickness and height.

The sample ID (Table 5) would correspond to the following nomenclature adopted for LOT by Clay Technology (see Figure 2): 13CNx.x for the North lower profile, 13ANx.x for the North

upper profile, 13ASx.x for the South upper profile, and 13CSx.x for the South lower profile, where x.x denotes the radial distance (in cm) from the heater surface to the middle of the sample.

Table 5: Sample labels and radial width of the subsamples of the N and S profiles

Position	Sample ID	Sample width	Sample ID	Sample width	Sample ID	Sample width	Sample ID	Sample width
		[mm]		[mm]		[mm]		[mm]
Heater	NL-1	12	NU-1	12	SL-1	11	SU-1	13
	NL-2	12	NU-2	14	SL-2	13	SU-2	15
	NL-3	14	NU-3	15	SL-3	13	SU-3	15
	NL-4	14	NU-4	15	SL-4	16	SU-4	15
	NL-5	12	NU-5	14	SL-5	15	SU-5	16
	NL-6	13	NU-6	12	SL-6	19	SU-6	15
	NL-7	11	NU-7	8	SL-7	8	SU-7	6
Outer rim	NL-8	6	NU-8	5				

4.3.2 XRD analysis

The samples used for XRD studies, as well as for cation exchange properties, wet and dry density, and for aqueous leaching analysis were cut from a profile oriented towards the West. The radial slab was cut in 4 radial segments, with the dimensions given as radial thickness in Table 6.

Table 6: Sample labels and radial width of the subsamples of the West profile

Orientation	Label	Length (mm)
Heater	W-1	12
	W-2	24
	W-3	30
Outer rim	W-4	30

The samples were cut with a small electric band-saw. Cutting was done through the plastic foil to minimize drying of samples (Figure 15). The cut segments are shown in Figures 16 and 17.

Whole-rock samples were powdered to a size approximately below 60 μm by gentle manual crushing in an agate mortar. The clay fraction ($< 2 \mu\text{m}$) was obtained from granulated material by sedimentation in a water column with an ammonium phosphate dispersant solution. Sedimentation time was extended to 18 and 72 hours using a column length of 20 cm.

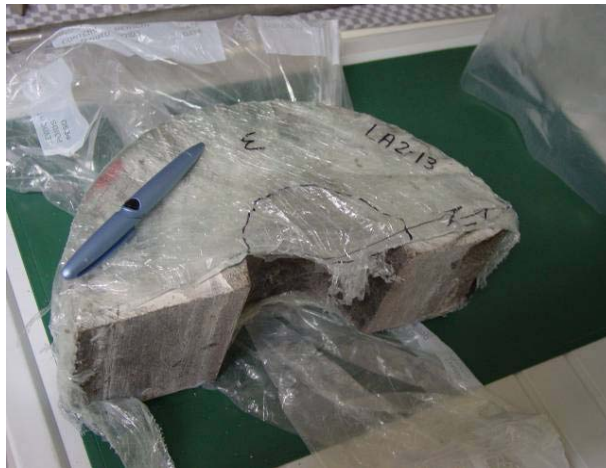


Figure 15: Western half of block 13 (LOT parcel A2) used to cut a vertical profile oriented towards the West (tip of pen)



Figure 16: Cut profile from block 13. The heater was in contact along the right side (curved surface), and the contact to granite was along the left side. The lower edge represents the base of block 13



Figure 17: Cut profile from block 13 after subsampling. The larger pieces were processed to perform the CEC, ion selectivity and XRD analyses. Some reference samples were kept sealed and refrigerated (for water content, density)

4.3.3 Wet and dry density

The density measurements had been conducted using the samples from the West profile. The samples were preserved from atmosphere in closed containers stored in a refrigerated room until measurement in order to minimize evaporation, and to preserve the original moisture content.

4.3.4 Aqueous leachates

Dried solid samples processed as described in Section 4.3.2 (XRD) were shaken in distilled water for two days, then filtered to $< 2 \mu\text{m}$. Different solid:liquid ratios were tested initially, and based on this, a S/L of 1:10 was used for all aqueous leachates.

4.3.5 Exchangeable cations

15 g of powdered rock material, previously air-dried at $105 \text{ }^\circ\text{C}$, was used and prepared in the same fashion as for XRD analysis (Section 4.3.2).

4.3.6 Cation exchange capacity by Na-acetate / Mg-nitrate displacement

The samples were previously dried for 48 hours at $105 \text{ }^\circ\text{C}$, whereby the cation exchange capacity in the clay can be referred to the dry sample mass. Samples were mildly ground manually in an agate mortar before processing.

4.3.7 Total carbon and sulfur

Approximately 2 g of gently ground (agate mortar) and dried sample (at $105 \text{ }^\circ\text{C}$) from the West profile were used to measure total and inorganic carbon as well as total sulfur.

5 Results

5.1 Water content

The water content was measured in 30 samples, corresponding to 2 different profiles carried out in duplicate (lower and upper sections), comprising 8 samples from the North Upper profile, 8 from the North Lower, 7 from the South Upper and 7 from the South Lower. The results have been plotted as function of the radial distance from the copper heater and also as function of drying time and temperature (see figures in Appendix A). 105 °C has been considered the reference temperature for dry mass of the samples. Water content relative to this temperature as reference is shown in Table 7.

Table 7: Water content relative to 105 °C and radial width of the subsamples of the N and S profiles

Profile	North Lower		North Upper		South Lower		South Upper	
Position	Sample width	Water content	Sample width	Water content	Sample width	Water content	Sample width	Water content
	[mm]	[wt%]	[mm]	[wt%]	[mm]	[wt%]	[mm]	[wt%]
Heater	12	27.5	12	27.8	11	27.5	13	27.6
	12	27.4	14	n.d.	13	27.3	15	27.4
	14	27.5	15	n.d.	13	27.3	15	27.4
	14	28.4	15	28.6	16	27.8	15	28.1
	12	30.0	14	30.5	15	29.2	16	29.7
	13	31.7	12	32.0	19	30.9	15	31.4
	11	33.2	8	33.3	8	32.0	6	31.7
Outer rim	6	33.5	5	33.0				

n.d.: not determined

The water content is lowest in the samples adjacent to the heater and is identical in all four Sections, 27.6 - 27.8 wt% relative to a dry mass determined at 105 °C. Towards the outer margin, water contents increase to 31.7 - 33.5 wt%, showing a slight asymmetry with the South profiles containing 1 - 2 wt% less water compared to the North profiles. The water content forms a plateau over the first inner 40 mm of radial section, and then is increasing in approximate linear fashion towards the margins. The sample closest to the heater in each profile contains consistently slightly more water than the adjacent samples to a distance of 40 mm.

The water loss as a function of temperature is increasing from that measured at 40 °C by 2 - 2.5 wt% to 105 °C, and only negligibly to a final temperature of 150 °C.

Additionally, the water content in samples W-3 and W-4 were determined in duplicate several months after measuring the North-South profile, to get a reference dry mass (105 °C) for the cation exchange capacity (CEC) measurements. Results are shown in Table 8. The measured

water content of the outermost sample (W-4) is consistent with the measurements of the more detailed N and S profiles documented above.

Table 8: Measured water content in samples W-3 and W-4 relative to 105 °C (/1 and /2 denote duplicates)

Sample	Water Content (%)
W-3/1	28.78
W-3/2	28.93
W-4/1	31.53
W-4/2	31.11

5.2 XRD analysis

The nomenclature adopted for the samples determined by XRD and some comments to clarify their treatment and origin are shown in Table 9. All diffractograms (Figures 32 - 44) are included in Appendix B.

Quartz, cristobalite and montmorillonite peaks have been detected in all samples. Likely feldspars were detected in one of the test samples (LOT-3.RD, Figure 32, Appendix B). The feldspars have been detected in a sample where a portion of the clay fraction had been removed (LOT-1.RD). Very small amounts of illite were detected in the test sample (fractions LOT-3.RD and LOT-4.RD, Figure 33, Figure 42, Appendix B). No new minerals have been formed above the detection limit of XRD. There were no special efforts made to optimize the detection of pre-existing of any newly formed accessory minerals.

Superposition of X-ray diffractograms made on sedimentary clay fraction samples at 18 and 72 hours (Figures 37 - 40, Appendix B) do not reveal any clear tendency on the clay behaviour as a function of the distance from the heater.

Na-montmorillonite is observed in all oriented clay samples (reference and profiles) but no Ca-montmorillonite has been detected.

Diffractograms of the bulk samples show some difference in peak asymmetry: samples W1, W3 and W4 look alike, but distinctly different from sample W2 and the unreacted reference sample for Block 13, with the latter two showing an asymmetry towards higher 2θ values. The interpretation of this feature is unclear: assuming that equal humidity prevailed (data recorded on the same day in an air-conditioned room) this might indicate that the samples with peaks shifted towards higher 2θ values represent more Na-rich montmorillonite. See Section 6 for further comments on this issue.

Table 9: Measured XRD samples

Sample	Profile location	Sedimentation time (h)	Figure, App. B	Remarks
REF-Bulk			32	LOT A2. Disoriented reference bulk sample for Block 13 (not subject to the LOT experiment)
REF-18.RD		18	34, 36	LOT A2. Oriented clay fraction of reference material for Block 13
REF-72.RD		72	35, 36	LOT A2. Oriented clay fraction of reference material for Block 13
LOT-1.RD		18	33	Oriented test sample, clay fraction
LOT-2.RD		24	33	Oriented test sample, clay fraction
LOT-3.RD			33	Oriented test sample. Residual sand and clay fraction taken after withdrawal of LOT-1.RD.
LOT-4.RD			33	Oriented test bulk sample without sedimentation.
w1-Bulk	W1		32	Disoriented bulk sample
w2-Bulk	W2		32	Disoriented bulk sample
w3-Bulk	W3		32	Disoriented bulk sample
w4-Bulk	W4		32	Disoriented bulk sample
W1-18.RD	W1	18	34, 40	Oriented sample, clay fraction
W2-18.RD	W2	18	34, 39	Oriented sample, clay fraction
W3-18.RD	W3	18	34, 38	Oriented sample, clay fraction
W4-18.RD	W4	18	34, 37	Oriented sample, clay fraction
W1-72.RD	W1	72	35, 40	Oriented sample, clay fraction
W2-72.RD	W2	72	35, 39	Oriented sample, clay fraction
W3-72.RD	W3	72	35, 38	Oriented sample, clay fraction
W4-72.RD	W4	72	35, 37	Oriented sample, clay fraction
LOT_Wnx.RD	W2,3,4		41, 42, 43, 44	Oriented dry sample, $n = 2,3,4$
LOT_Wny.RD	W2,3,4		41, 42, 43	Oriented sample saturated in ethyleneglycol
LOT_Wnz.RD	W2,3,4		41, 42, 43	Oriented sample heated at 550 °C for 2 hours

5.3 Wet and dry density

The bulk wet density of the West profile was measured. From the obtained values, the bulk dry density was calculated from the measured water content, and the average values are summarized in Table 10.

Table 10: Measured Bulk Densities

Sample ID	Bulk wet density (g/cm ³)	Bulk dry density (g/cm ³)
W-1	1.92	1.51
W-2	1.95	1.52
W-3	1.93	1.46
W-4	1.89	1.42

The value of bulk dry density varies between 1.42 and 1.52 g/cm³. The lower densities are measured in the samples farther away from the heater (sample W-4) which also contain more water compared to those from near the heater. Consequently, values of bulk dry density are higher close to the heater. The distribution of the bulk density (packing of the rock particles in samples) along the profile is in accordance with the water content along the profile (Table 7).

5.4 Aqueous leachates

The aqueous leachates are dominated by sodium, chloride and sulfate, which is typical for a montmorillonite. Sample W-2 displays anomalously high concentrations of Na and SO₄ as well as K, Ca and Mg (Figure 18). The charge balance for the elevated cation concentrations is mainly compensated by sulfate. Chloride displays a regular distribution, increasing slightly from the heater towards the outer margin. The concentrations on the outermost sample are lower for all ions compared to the unreacted reference sample for Block 13 with the exception of chloride. The seemingly anomalously high concentrations found in sample W-2 are confirmed by the measurements in duplicate. All measured concentrations in aqueous leachates are shown in Appendix C.

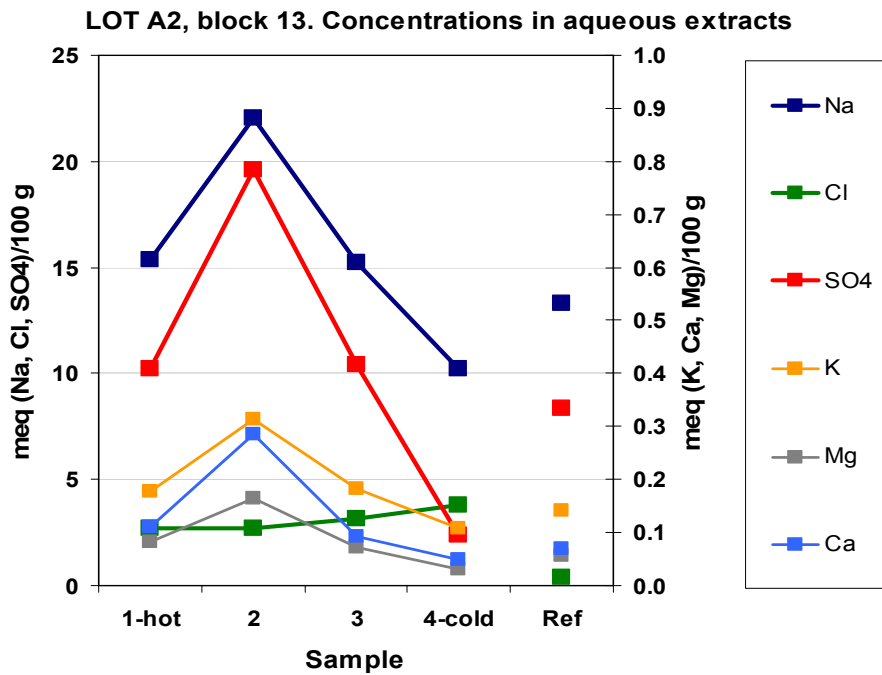


Figure 18: Aqueous species distribution in the aqueous leachates as function of their proximity to the cooper heater (meq/100 g dry mass)

5.5 Exchangeable cations

The cations measured as exchangeable must be corrected for cations originating from dissolution of soluble salts (residues from dried porewater and / or accessory minerals) to obtain “true” values. Bradbury and Baeyens (1998) proposed two cases to estimate the in situ cation occupancies. As case I, they considered to combine all chloride measured in the aqueous leachates with sodium and all sulfate with calcium and conceive these concentrations as a result of dissolution of the salts sodium chloride and calcium sulfate. As case II, they considered to combine both, chloride and sulfate, with sodium, and subtracting equivalent amounts from the exchangeable sodium. Potassium, magnesium and strontium extracted with the nickel method and measured by AAS are considered to maintain the same concentration without any correction.

Following this argument, data applying a correction according to cases I and II are presented in Table 11. All samples are reported in duplicate analysis (/1 and /2). The 0.5 in the sample label refers to the solid:liquid ratio used. Ni LOT A2-13 is the reference material. The uncorrected values for the concentrations of the exchangeable cations are listed in Appendix D.

Table 11: Corrected distribution of exchangeable cations (meq/100 g dry mass)

Sample	Correction case I: NaCl/CaSO ₄							Correction case II: NaCl/Na ₂ SO ₄						
	Ca	Na	Mg	K	Sr	Cu	Total	Ca	Na	Mg	K	Sr	Cu	Total
Ni LOT A2-13 0.5/1	8.7	57.7	4.2	1.4	0.5	N.D.	72.5	17.0	49.4	4.2	1.4	0.5	N.D.	72.5
Ni LOT A2-13 0.5/2	9.1	57.7	4.1	1.4	0.5	N.D.	72.8	17.5	49.3	4.1	1.4	0.5	N.D.	72.8
Ni W-1B 0.5/1	15.1	52.7	6.1	1.3	0.5	1.64	77.3	25.0	42.9	6.1	1.3	0.5	1.64	77.3
Ni W-1B 0.5/2	14.4	52.5	6.3	1.3	0.5	1.63	76.6	25.0	41.9	6.3	1.3	0.5	1.63	76.6
Ni W-2B 0.5/1	8.0	56.4	5.1	1.5	0.5	1.51e-2	71.5	27.7	36.7	5.1	1.5	0.5	1.51e-2	71.5
Ni W-2B 0.5/2	7.8	56.6	5.1	1.5	0.5	1.52e-2	71.5	27.3	37.1	5.1	1.5	0.5	1.52e-2	71.5
Ni W-3B 0.5/1	12.1	55.9	5.0	1.4	0.5	1.49e-3	74.9	23.0	45.0	5.0	1.4	0.5	1.49e-3	74.9
Ni W-3B 0.5/2	13.0	56.0	5.1	1.4	0.5	1.53e-3	76.0	22.8	46.1	5.1	1.4	0.5	1.53e-3	76.0
Ni W-4B 0.5/1	13.8	56.8	5.5	1.3	0.5	6.98e-2	78.0	16.2	54.4	5.5	1.3	0.5	6.98e-2	78.0
Ni W-4B 0.5/2	13.9	55.9	5.3	1.3	0.4	5.05e-2	76.9	16.2	53.6	5.3	1.3	0.4	5.05e-2	76.9

N.D. = not detectable

The results for the corrected values applying both cases, I and II, are shown in Figure 19, displaying only the major cations Ca, Na, Mg and K:

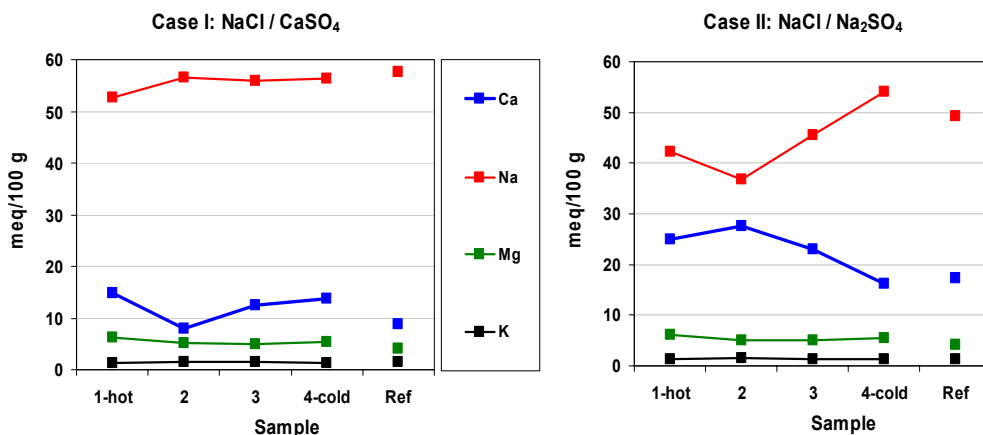


Figure 19: Distribution of exchangeable cations as a function of sample position relative to the copper heater for case I (Na corrected for aqueous Cl equivalents and Ca for aqueous SO₄) and case II (Na corrected for aqueous Cl + SO₄ equivalents)

Cu was also measured in the extracted Ni solutions. It was found to be below a detection limit of 10⁻³ meq/100g in the reference sample, but was measurable in all samples of the profile. Highest values of 1.6 meq/100g were found adjacent to the Cu-heater, decreasing to a minimum of 1.5·10⁻³ meq/100g in sample W-3 and increasing again to ~ 6·10⁻² meq/100g at the margin

adjacent to the granite. The measurements are corrected for a small blank of Cu concentration contained in the Ni solution. The data are tabulated in Appendix D.

5.6 Sum of measured exchangeable cations

The sum of exchangeable cations in equivalents (81 - 94 meq/100 g) is ~ 21.5 % less than the Ni consumption (107 - 116 meq/100 g). The data is presented in Appendix D. The sum of the exchangeable cations is listed in Table 11 and is shown in Figure 20. Because the correction is based on milliequivalents, the total value is the same in both cases.

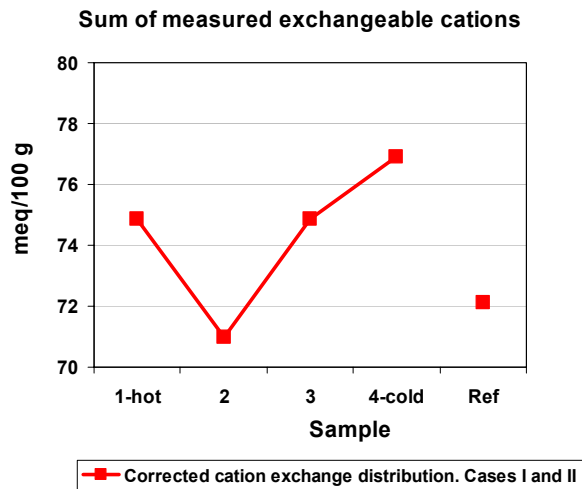


Figure 20: Sum of measured exchangeable cations as function to the sample position relative to the copper heater applying corrections (cases I and II) as described above

5.7 Cation exchange capacity determined by Na/Mg displacement

The total CEC measured in duplicate by the Na-Mg displacement method in the samples of the West profile is shown in Table 12. The value obtained for the reference material from Block 13 does agree very well with the sum of the measured exchangeable cations after correction (cases I and II, above).

In addition, aqueous calcium was measured in the final magnesium nitrate solution. Results just confirm the dissolution of significant calcite and / or gypsum / anhydrite, but the calcium concentration measured is not conclusive because some of this calcium may have been retained from previous extraction steps with sodium acetate, and also because some calcite might remain in bentonite to be continuously dissolved. Calcium measured in solution is also shown in Table 12.

The results of the direct CEC measurements are compared in Figure 21 with the sum of the exchangeable cations after correction for Cl^- and SO_4^{2-} .

Table 12: Cation exchange capacity and calcium dissolved from calcite (meq/100 g)

Sample	CEC (meq/100 g)	Ca ²⁺ (meq/100 g)
Ni LOT A2-13 0.5/1	71.6	14.7
Ni LOT A2-13 0.5/2	71.3	14.7
Ni W-1B 0.5/1	72.1	14.3
Ni W-1B 0.5/2	71.5	14.2
Ni W-2B 0.5/1	70.0	14.1
Ni W-2B 0.5/2	73.6	14.0
Ni W-3B 0.5/1	74.6	14.9
Ni W-3B 0.5/2	73.5	15.3
Ni W-4B 0.5/1	74.1	14.9
Ni W-4B 0.5/2	74.4	14.8

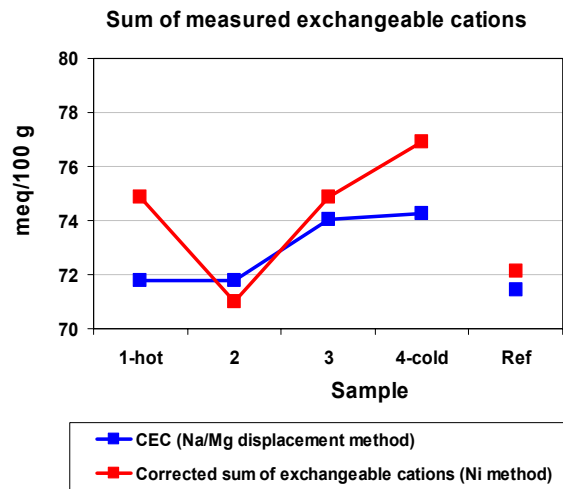


Figure 21: Comparison between the sum of measured exchangeable cations by the Ni(en) method (average of duplicate analyses) and the cation exchange capacity measured by the Na/Mg displacement method related to the sample position from the copper heater

5.8 Total carbon and sulfur

Results of total, inorganic and organic carbon and total sulfur are shown in Table 13. These values transformed to equivalents per 100 g are used further in the discussion.

Table 13: Total, inorganic and organic carbon and total sulfur on the West profile samples

Sample	Total C (%)	Inorganic C (%)	Organic C (%)	Total S (%)
LOT A2-13 0.5/1	0.6	0.6		0.3
LOT A2-13 0.5/2	0.7	0.6	< 0.1	0.3
W-1B 0.5/1	0.9	0.6		0.4
W-1B 0.5/2	0.9	0.6	0.3	0.4
W-2B 0.5/1	0.4*	0.4*		0.5
W-2B 0.5/2	0.7	0.5	0.1	0.5
W-3B 0.5/1	0.5	0.5		0.3
W-3B 0.5/2	0.5	0.5	< 0.1	0.2
W-4B 0.5/1	0.6	0.5		0.2
W-4B 0.5/2	0.5	0.5	< 0.1	0.2

* Possibly below a detection limit of 0.5 wt. %. Organic C is computed by difference.

In accordance with the observed distribution in the aqueous sulfate, the total amount of sulfur present in the second sample (W-2) is significantly higher than the rest of the sections. The detection limit for the sulfur content is ~ 0.1 wt%.

Although the detection limit for C by the method used might be better than 0.5 wt% for carbonate-poor materials, such as the MX-80 bentonite, the unexpected relatively high amount of organic carbon (by difference) in the section closest to the heater (W-1) is most likely not significant because of the large combined errors.

6 Comments and discussion

An in-depth discussion of optimal analytical procedures and the analytical results will be part of a collaborative effort of the partners involved in the LOT experiment and the analysis of parcel A2. The following sections contain a brief discussion just of the data of this report. By the same reason, the discussion is limited in some cases because results from other studies are not included at this stage.

6.1 Water content

In general, the water content is decreasing as a function of the proximity to the heater. It can be observed in Figures 5-A to 9-A (Appendix A) that the water content distribution in Sections 2 and 3 (11 to 40 mm from the copper heater) in all profiles is slightly lower than the water content in the section immediately adjacent to the heater. This anomaly could have been caused during the cooling of the parcel after turning off the heater, combined with either a re-distribution of water, or an external source of water. The effect of volume contraction during cooling may also be significant to consider, and this would be more significant for samples close to the heater.

In terms of temperature effect on drying, most of the water is lost up to 70 °C. Small losses are observed from 70 to 150 °C. A reference temperature of 105 °C appears reasonable for relating data to dry mass. The important point is that samples – especially small blocks – have to be dried until a constant mass is reached rather than just for a fixed duration of time (e.g. 24 hrs).

6.2 XRD analysis

There is no difference observed in the oriented XRD patterns of the clay fraction – the clay material appears to be unchanged in comparison to the reference sample regardless of grain size and position relative to the heater. The idea was to separate and compare a very fine grained clay fraction (72 hrs) because this fraction would presumably be the most sensitive one to display any effects of thermal modification.

The differences observed in the disoriented bulk samples of the West profile compared to the reference sample (diffractogram 1, Appendix B) in the 5 - 10 °2θ region need to be further discussed. It is striking that sample W2 is more like the unreacted bulk sample of Block 13, compared to the three other samples of the profile (Figure 32, Appendix B). This correlates with lower Ca-contents in the exchangeable cation populations in the former two samples (see details below). It can therefore be inferred that the reference sample and sample W2 should be more Na-montmorillonite rich compared to the other samples of the profile. This would result in a peak shift towards higher 2-theta values as observed.

6.3 Wet and dry density

The measured wet density of 1.92 - 1.95 g/cm³ adjacent to the heater is somewhat lower than that reported by Clay Technology on nearby Blocks 15 and 11 as 1.98 g/cm³ (Table 3). The value measured for a sample at the cold end of the profile is 1.89 g/cm³ and compares to values of 1.91 - 1.92 g/cm³ from blocks 15 and 11 (data by Clay Technology). It should be noted that Clay Technology determined densities shortly after sampling.

It should be noted that it was not planned to measure densities systematically for this study. The measurements represent a mere test for the paraffin oil immersion method and were carried out several month after sampling on samples that had been kept in closed containers in cold storage, but that may have undergone some volumetric relaxation. Nevertheless, the agreement is reasonable, but the density data for the samples of this study should not be used to calculate a degree of saturation. Instead, the degree of saturation for Block 13 should be assumed to be similar to that determined for nearby Blocks 15 and 11 by Clay Technology.

6.4 Aqueous leachates

The distribution of the cations and anions displayed in the profile of aqueous leachates is not straightforward to interpret, in particular the seemingly anomalously high SO_4 content in sample W-2 (and associated elevated Na and Ca concentrations). The underlying Block 12 did contain heterogeneous packages of anhydrite (10 %, as discrete embedded plugs), and this may have locally influenced the sulfate content in the overlaying Block 13. It may also be plausible, that heterogeneities in the content of accessory sulfate minerals do exist. This issue was not further resolved within the scope of this project, but could be addressed by analyzing additional profiles in a different orientation. The observations on this profile are, however, in agreement with studies by other partners that also document a sulfate accumulation towards the hot part of the profile.

6.5 Exchangeable cations and sum of cations

The appearance of the profile of the measured exchangeable cations is strongly influenced by the anomalously high sulfate concentration and its associated correction to the exchangeable cations, either to Na and Ca (case I) or only Na (case II). The favored correction is that of associating Cl concentrations with Na, and sulfate concentrations with Ca. The “true” correction may be a mixed correction composed of the two end-members, I and II. The existence of the low Ca population on the exchanger in sample W-2 is therefore uncertain, and should be confirmed with additional measurements.

The chloride profile shows an increase towards the outer margin as may be expected from contact with the saline groundwater. The values (and those of the other ions) should be compared to the actual composition of the infiltration groundwater to the LOT Parcel A2.

By reasons not yet determined, the sum of exchangeable cations in equivalents (81 - 94 meq/100 g) is ~ 21.5 % less than the Ni consumption (107 - 116 meq/100 g). Proton exchange on permanent charge sites hasn't been measured, but this is not expected to be significant enough to explain this discrepancy due to the small surface area for edge sites ($8.5 \text{ m}^2/\text{g}$) compared to the total surface area ($788 \text{ m}^2/\text{g}$) in a compacted Na-MX-80 clay fraction studied by Tournassat et al. (2004). This same discrepancy between the sum of exchangeable cations and the exchange capacity was described by Bradbury and Baeyens (1998) for Opalinus clay core samples drilled up to 20 m into the wall rock of a reconnaissance gallery associated with the Mont Terri motorway tunnel in Canton Jura, Switzerland.

The sum of the exchangeable cations corrected for by case I or II varies along the profile with a tendency to be slightly higher values by less than 2 meq/100g on average compared to the reference sample, with the exception of sample W-2. Such a variation is, however, within the combined analytical uncertainties. There is therefore no significant change in the exchange capacity evident between the reference sample and those of the hot zone of the LOT Parcel A2.

The presence of Cu (1.6 meq/100g) measured in the sample adjacent to the heater is not surprising. It is notable, however, that small concentrations of Cu were measured throughout the profile that were distinctly higher compared to the reference material for Block 13. The increased value for Cu in the outermost sample can be reasoned by the presence and corrosion of many CuNi tubes along the bentonite-bedrock interface used for protection of the electric connections to the sensors (see Figure 4, for example). It has not been demonstrated if the Cu is present entirely on the exchanger, or as a secondary precipitate. This could probably have been achieved by doing additional extracts with formic acid that would dissolve any residual Cu-phase. It may also be possible that Cu present on the exchanger may enter the octahedral sheet at elevated temperature. This would modify the layer charge (small change). If this could be detected by measurements is questionable.

6.6 Cation exchange capacity by Na/Mg displacement

The Na/Mg method may underestimate the CEC for at least two reasons: (1) small amounts of the finest size fraction may be lost during repeat decanting (likely not significant), and (2) any calcite or Ca-sulfate dissolution occurring during the Na-acetate exchange may leave some Ca on the exchanger despite repeat exchange steps. Ca-phases did clearly and significantly dissolve during the last step of the repeat Mg-nitrate displacement, as was seen by the measured Ca concentrations (Table 12).

The reproducibility between the duplicate samples is excellent and the data set does show a slight tendency in the distribution of the total cation exchange capacity to increase by ~ 2 meq/100g from the heater towards the outer rim, but again, this is within the combined analytical uncertainty.

The CEC values obtained by direct measurement (Na-acetate / Mg-nitrate) agree very well with the sum of the exchangeable cations (Ni-en, corrected) for samples W-2, W-3 and the reference. This is providing confidence in the two methods and supports the assumptions underlying the corrections applied to the sum of the cations based on the anion concentrations obtained by the aqueous extracts. The sum of the cations is approximately 3 meq/100g larger compared to the CEC for samples W-1 and W-4. The combined measurement uncertainties are estimated to about 4 % relative, equivalent to 2.9 meq/100g at a level of 72 meq/100g.

We may therefore conclude that the two methods employed for estimating the CEC are largely in agreement, and that the CEC did not change significantly during the experiment in Block 13. The possible slight increase permitted by the data would have to be substantiated by a large data set, and some more testing of the individual steps of the analytical procedures.

6.7 Carbon and sulfur

The measurement values obtained for inorganic carbon and total sulfur, as well as the amount of calcium, chloride, sulfate and alkalinity (as CO_3^{2-}) extracted in the aqueous leaches, and the exchangeable calcium have been transformed to equivalents, assuming 100 g of dry sample mass (Table 14). Total inorganic carbon and sulfur and aqueous CO_3^{2-} and SO_4^{2-} are also plotted in Figure 22 to compare the values and discuss some assumptions on the reactivity of accessory mineral phases in bentonite.

It is observed that the amount of sulfate extracted in the aqueous leachates has a similar distribution as the total amount of sulfur determined in the bulk sample, arising from accessory sulfates and minor dissolved sulfate. It is therefore reasonable to infer that hydrated (e.g. gypsum,

bassanite) or dehydrated CaSO_4 (anhydrite) and possibly also Na_2SO_4 (residual of dried pore-water) are dissolving relatively rapidly during aqueous extractions until complete dissolution or saturation. These observations are in support of associating Ca^{2+} with SO_4^{2-} when performing the corrections on the determinations of exchangeable cations.

Table 14: Averaged values of duplicates of the West profile: aqueous and exchangeable calcium, inorganic and aqueous carbon (as CO_3^{2-}), total and aqueous sulfur (as SO_4^{2-}) and aqueous chloride. All values relate to 100 g of dry sample

Sample	Aqueous Ca (eq)	Exchang. Ca (eq)	Inorg. C or CO_3^{2-} (eq)	Alkalinity as CO_3^{2-} (eq)	Total S or SO_4^{2-} (eq)	Aqueous SO_4^{2-} (eq)	Aqueous Cl (eq)
LOT ref.	2.3E-04	1.7E-02	1.0E-01	8.7E-03	1.9E-02	8.4E-03	4.0E-04
W-1	3.7E-04	2.5E-02	1.0E-01	5.2E-03	2.5E-02	1.0E-02	2.7E-03
W-2	9.5E-04	2.8E-02	7.5E-02	3.2E-03	3.1E-02	2.0E-02	2.7E-03
W-3	3.0E-04	2.3E-02	8.3E-02	4.4E-03	1.6E-02	1.0E-02	3.1E-03
W-4	1.6E-04	1.6E-02	8.3E-02	6.9E-03	1.3E-02	2.4E-03	3.8E-03

In contrast to sulfur, the total inorganic carbon is one order of magnitude higher compared to the dissolved carbon (measured as alkalinity) in the aqueous extracts. There is evidence of substantial dissolution of calcite during the CEC measurement (Ca^{2+} measured in the CEC MgNO_3 solution), but for the aqueous extracts the dissolution of calcite is much smaller than that for Ca-sulfate. The solutions used during the Ni-en exchange for obtaining exchangeable cations are pH-buffered to minimize calcite dissolution.

While it may be possible that different amounts of gypsum and calcite are dissolving during aqueous extraction and the exchange procedures, the consistency of the direct CEC determination and the sum of exchangeable cations (after corrections) lend support to the method and justifications adopted here.

Some other combinations for applying corrections to the exchangeable cations may also be envisaged – but cannot be further constrained or evaluated by the data available.

The presence of significant amounts of carbonates and sulfates in bentonite suggests that equilibrium with respect to calcite and gypsum in the pore solution may be established after bentonite saturation. These accessory phases will also form significant inventories of anions and cations, as well as buffering capacity (calcite) during porewater-bentonite interaction. The amounts of aqueous chloride are also relatively high (Table 14), suggesting the presence of soluble salts and / or impurities.

Relatively little emphasis was placed in the past on tracking and using the mineralogical changes of the accessory minerals during long-term laboratory and field experiments on compacted bentonite systems. The authors suggest that it would be important to more carefully examine the role and nature of the accessory minerals as these will exert an important control on the evolution of porewater chemistry and related mass transfer processes.

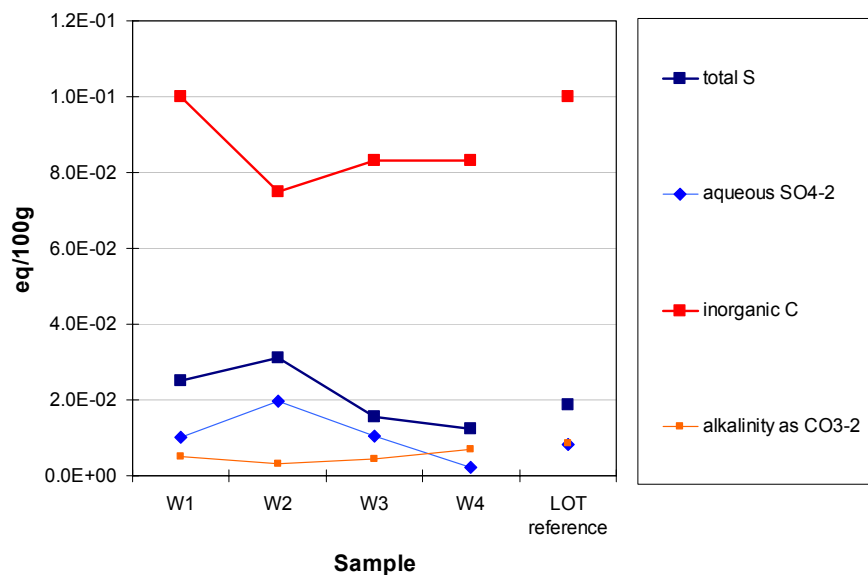


Figure 22: Inorganic and aqueous carbon (soluble as CO_3^{2-}) and total and aqueous sulfur (soluble as SO_4^{2-}) distribution related to the sample position from the copper heater

6.7 Additional issues

The possibility of any textural changes of the compacted bentonite has not been addressed in this study. Generally, it is assumed that compacted bentonite will largely behave as a homogeneous medium after full saturation. Cementation effects as a result of thermal gradients may, however, affect very locally grain distribution, porosity distribution, surface area, water uptake, and swelling properties.

6.8 Recommendations

The presence of relatively sharply bound chemical heterogeneities (sample W2 of the West profile, and observed by other investigators as well) as evident in the cation occupancy must also link to variations in the content and distribution of accessory minerals. It is therefore important from a geochemical point of view to better characterize these heterogeneities as these are likely to exert chemical controls on porewater composition, and hence, also mass transport and local swelling behavior. This would require the application of optimized non-aqueous separation methods to increase the resolution of XRD methods, and also to perform further studies on the separated material.

Acknowledgments

The authors like to acknowledge the excellent management of the LOT Project by Clay Technology (Ola Karnland). Hanspeter Weber and Paul Wersin of Nagra initiated and financed this project. Michael Plötze (ETH Zürich) kindly reviewed a draft version and provided many comments and suggestions. Ruth Mäder (RWI, University of Bern) performed the CEC determinations and aqueous extracts. Analytical work was supported by the teams of Urs Eggenberger (XRD) and Niklaus Waber (IC analytics) at RWI, University of Bern. Martin Mazurek and Niklaus Waber (RWI, University of Bern) contributed to the data interpretation.

References

- Bradbury, M.H. & Baeyens, B., 1998. A Physicochemical Characterisation and Geochemical Modelling Approach for Determining Porewater Chemistries in Argillaceous Rocks. *Geochimica et Cosmochimica Acta* 62, 783-795.
- Karnland, O. & Birgersson, M., 2006. Montmorillonite stability, with special respect to KBS-3 conditions. SKB Technical Report TR-06-11.
- Newman, A.C.D. & Brown, G., 1987. The Chemical Constitution of Clays, Mineralogical Society Monograph No.6, ed. A.C.D. Newman, 1987.
- Tournassat, C., Greneche, J.-M., Tisserand, D. & Charlet, L., 2004. The titration of clay minerals: I. Discontinuous backtitration technique combined with CEC measurements. *Journal of Colloid and Interface Science*, 273, 224-233.
- Rhoades, J.D., 1982. Cation Exchange Capacity. A.L. Page, R.H. Miller and D.R. Keeney Eds., *Methods of Soil Analysis, Part 2. Chemical and Microbiological Properties*. ASA-SSSA, Madison, Wisconsin, USA, 2nd ed, 149-157 pp.

Appendix A - Water content data

Water content measurements of Block 13 of Parcel A2 of the LOT Experiment are summarized in Tables 15 and 16 and depicted in Figures 23 - 31.

Table 15: Water content as a function of temperature and distance from the copper heater in the North profile (Lower and Upper)

Water content [mass ratio] in profile "North Lower"					Water content [mass ratio] in profile "North Upper"				
distance (mm)	40 °C	70 °C	90 °C	105 °C	distance (mm)	40 °C	70 °C	90 °C	105 °C
0 - 12	0.258	0.271	0.273	0.275	0 - 12	0.260	0.274	0.276	0.278
12 - 24	0.259	0.270	0.272	0.274	12 - 26	n.d.	n.d.	n.d.	n.d.
24 - 38	0.260	0.271	0.273	0.275	26 - 40	n.d.	n.d.	n.d.	n.d.
38 - 52	0.270	0.281	0.283	0.284	40 - 55	0.272	0.283	0.285	0.286
52 - 65	0.287	0.297	0.299	0.300	55 - 69	0.292	0.302	0.304	0.305
65 - 77	0.304	0.314	0.316	0.317	69 - 81	0.307	0.317	0.319	0.320
77 - 89	0.319	0.329	0.331	0.332	81 - 90	0.320	0.330	0.332	0.333
89 - 95	0.324	0.332	0.334	0.335	90 - 95	0.318	0.327	0.328	0.330

n.d.: not determined

Table 16: Water content as a function of temperature and distance from the copper heater in the South profile (Lower and Upper)

Water content [mass ratio] in profile "South Lower"					Water content [mass ratio] in profile "South Upper"				
distance (mm)	40 °C	70 °C	90 °C	105 °C	distance (mm)	40 °C	70 °C	90 °C	105 °C
0 - 11	0.258	0.271	0.273	0.275	0 - 13	0.258	0.272	0.274	0.276
11 - 24	0.257	0.269	0.272	0.273	13 - 28	0.256	0.270	0.272	0.274
24 - 38	0.258	0.270	0.272	0.273	28 - 43	0.258	0.270	0.272	0.274
38 - 53	0.264	0.274	0.276	0.278	43 - 58	0.266	0.278	0.279	0.281
53 - 68	0.278	0.289	0.290	0.292	58 - 74	0.284	0.294	0.296	0.297
68 - 87	0.292	0.306	0.307	0.309	74 - 89	0.300	0.311	0.313	0.314
87 - 95	0.308	0.317	0.319	0.320	89 - 95	0.305	0.314	0.316	0.317

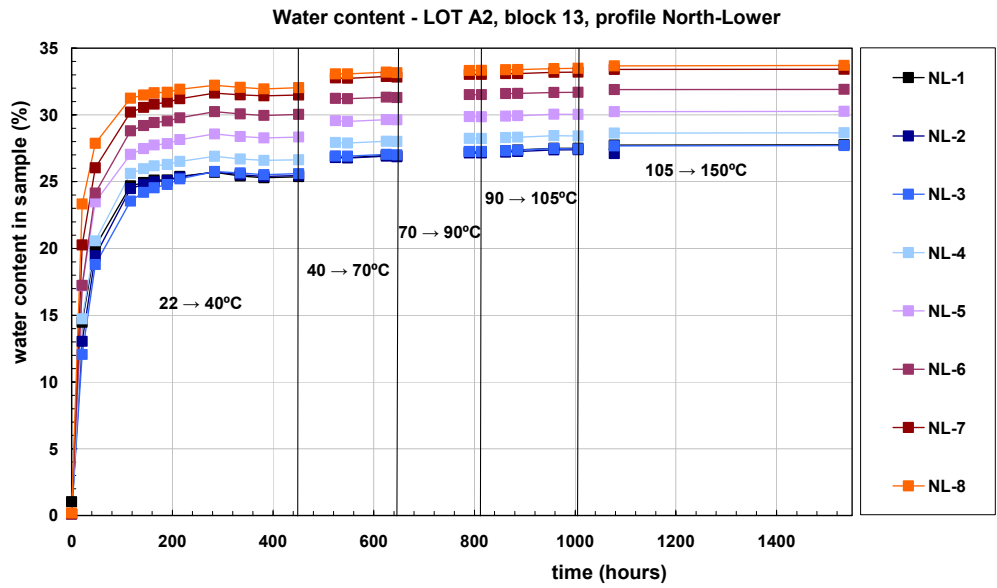


Figure 23: Water content in the North-Lower profile as a function of time of drying and drying temperature augmented incrementally

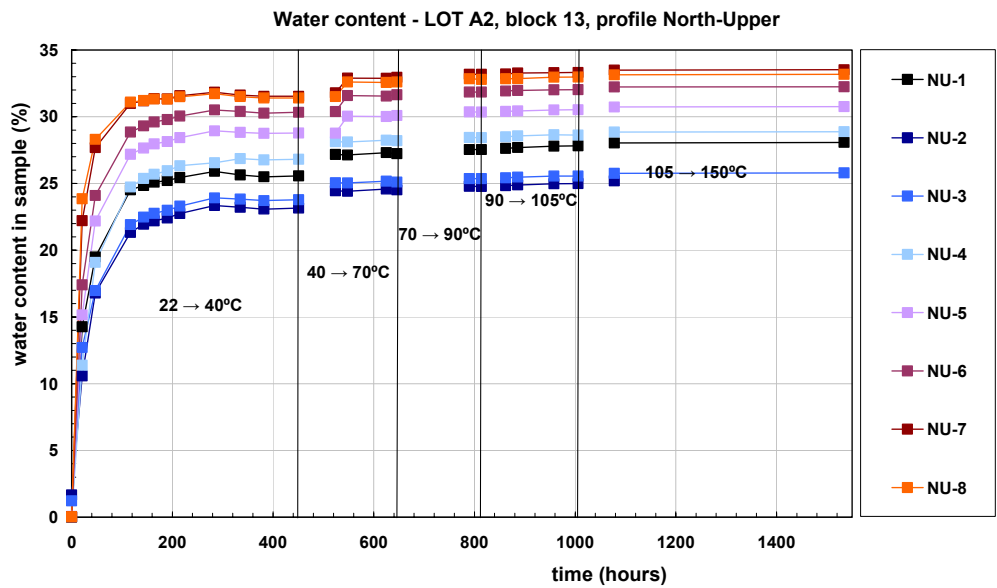


Figure 24: Water content in the North-Upper profile as a function of time of drying and drying temperature augmented incrementally

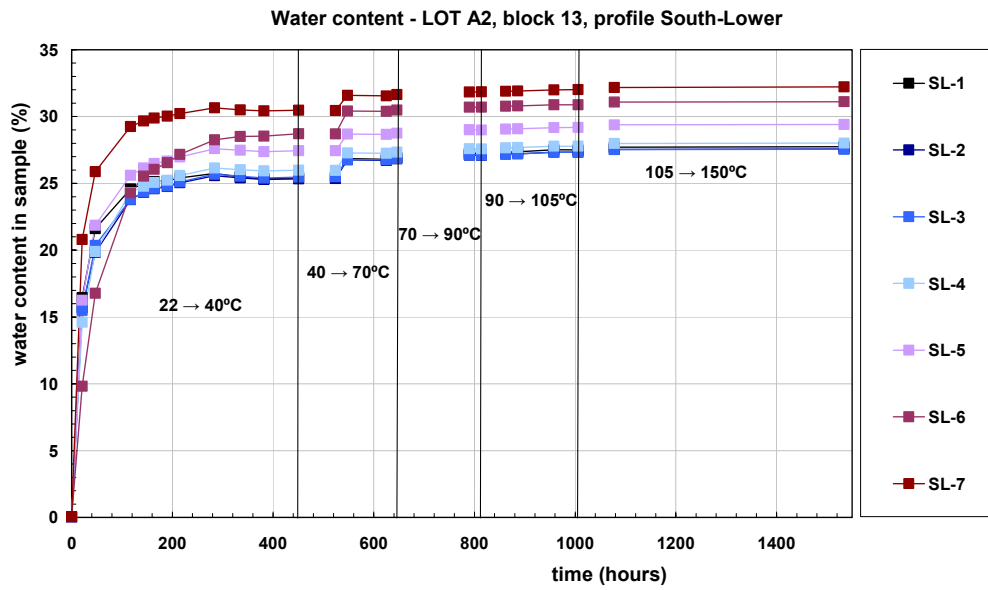


Figure 25: Water content in the South-Lower profile as a function of time of drying and drying temperature augmented incrementally

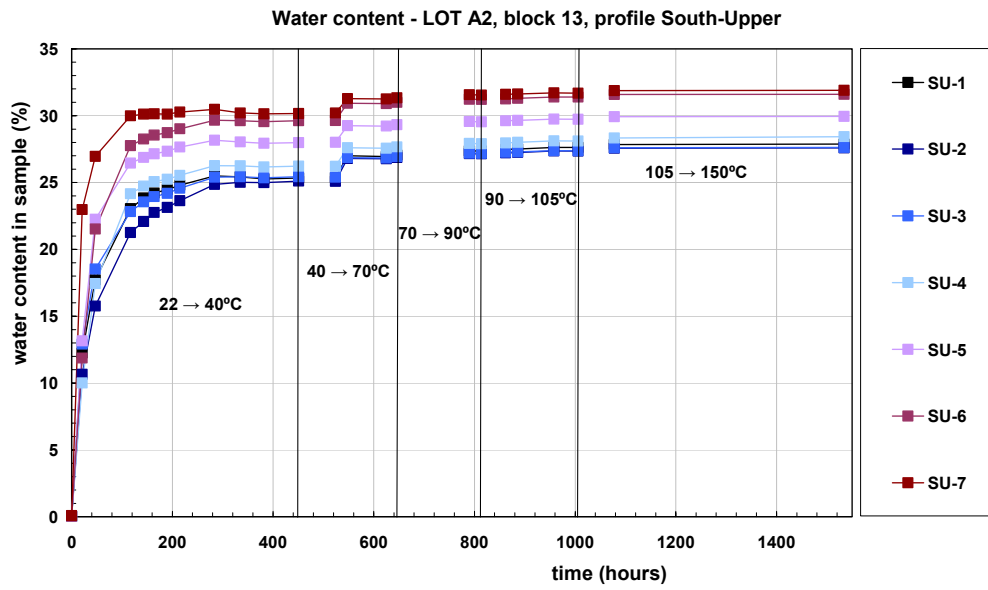


Figure 26: Water content in the South-Upper profile as a function of time of drying and drying temperature augmented incrementally

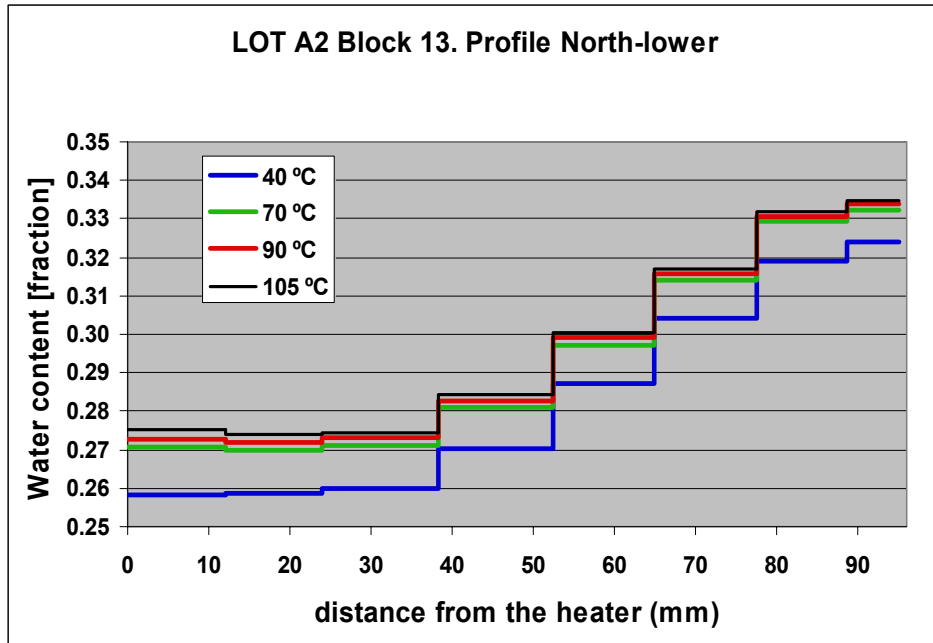


Figure 27: Water content at selected temperatures in the North-Lower profile in function of the distance from the heater

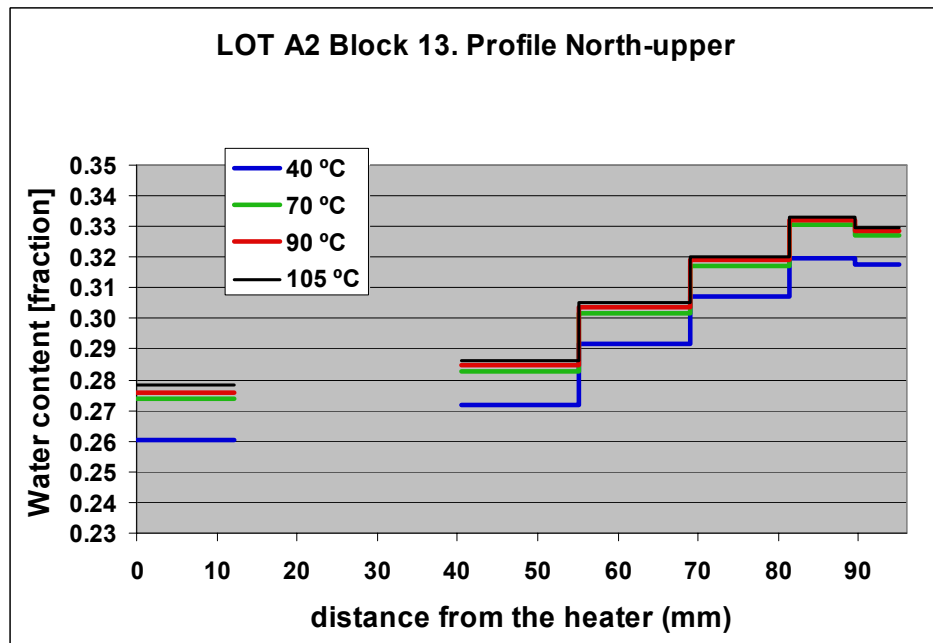


Figure 28: Water content at selected temperatures in the North-Upper profile in function of the distance from the heater

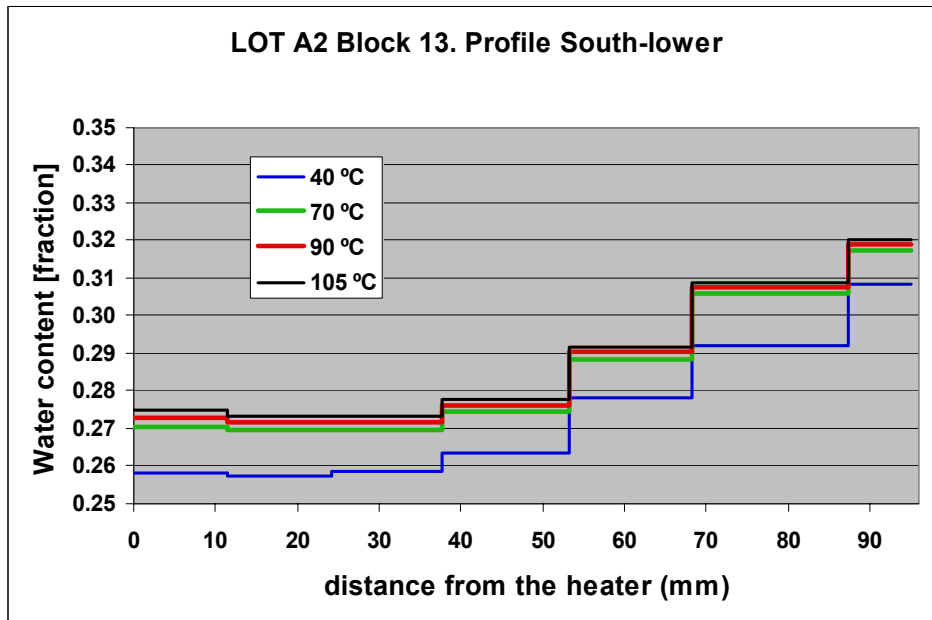


Figure 29: Water content at selected temperatures in the South-Lower profile in function of the distance from the heater

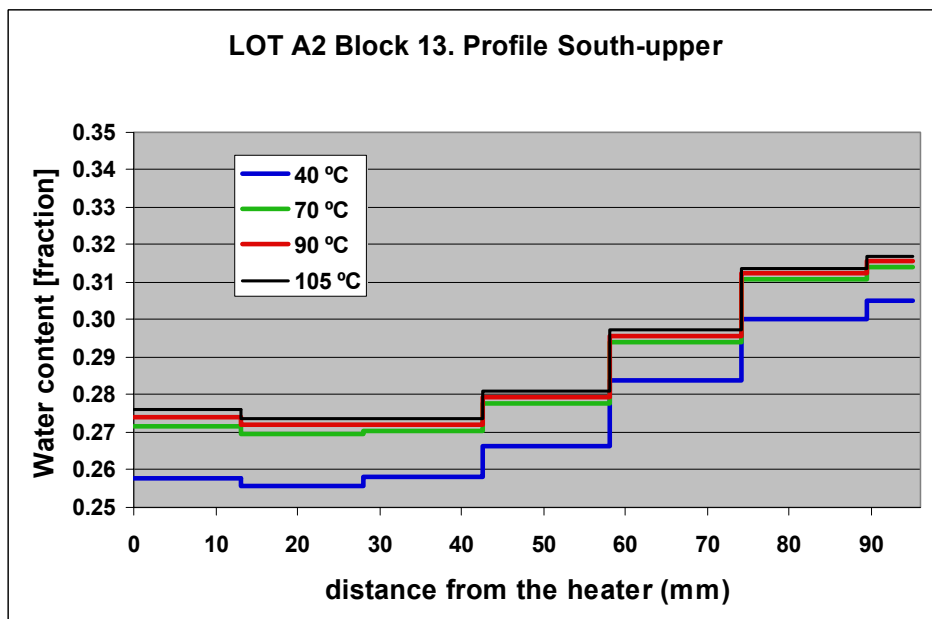


Figure 30: Water content at selected temperatures in the South-Upper profile in function of the distance from the heater

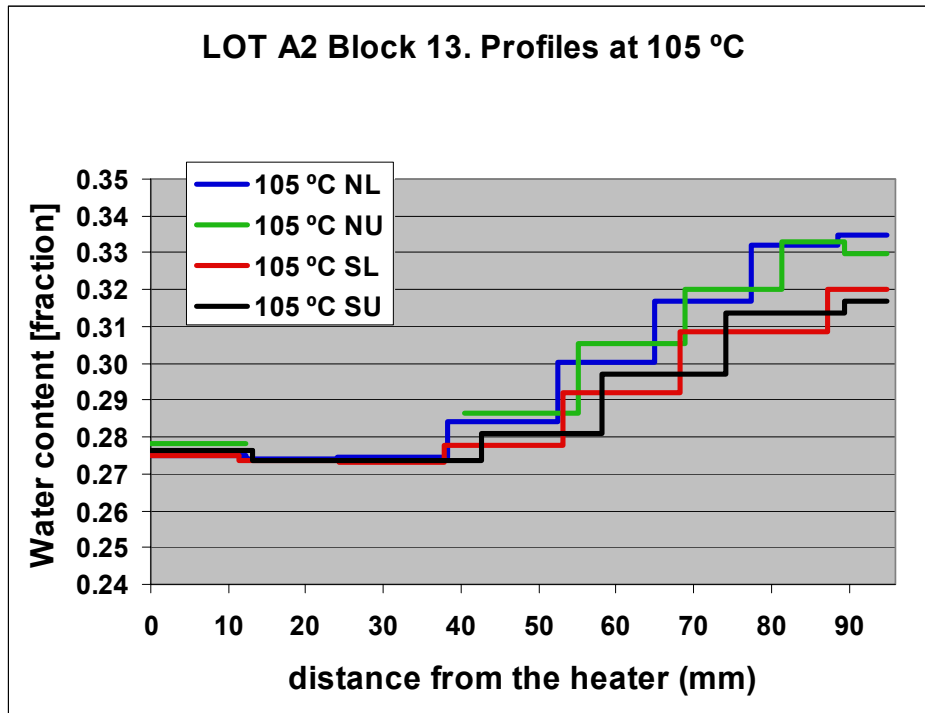


Figure 31: Comparison of the water content in all profiles at 105 °C, in function of the distance from the heater

Appendix B - XRD data

The XRD patterns are displayed in Figures 32 - 44. See Table 9 for a summary and overview of samples and sample preparation.

B-8

NAGRA NAB 08-08

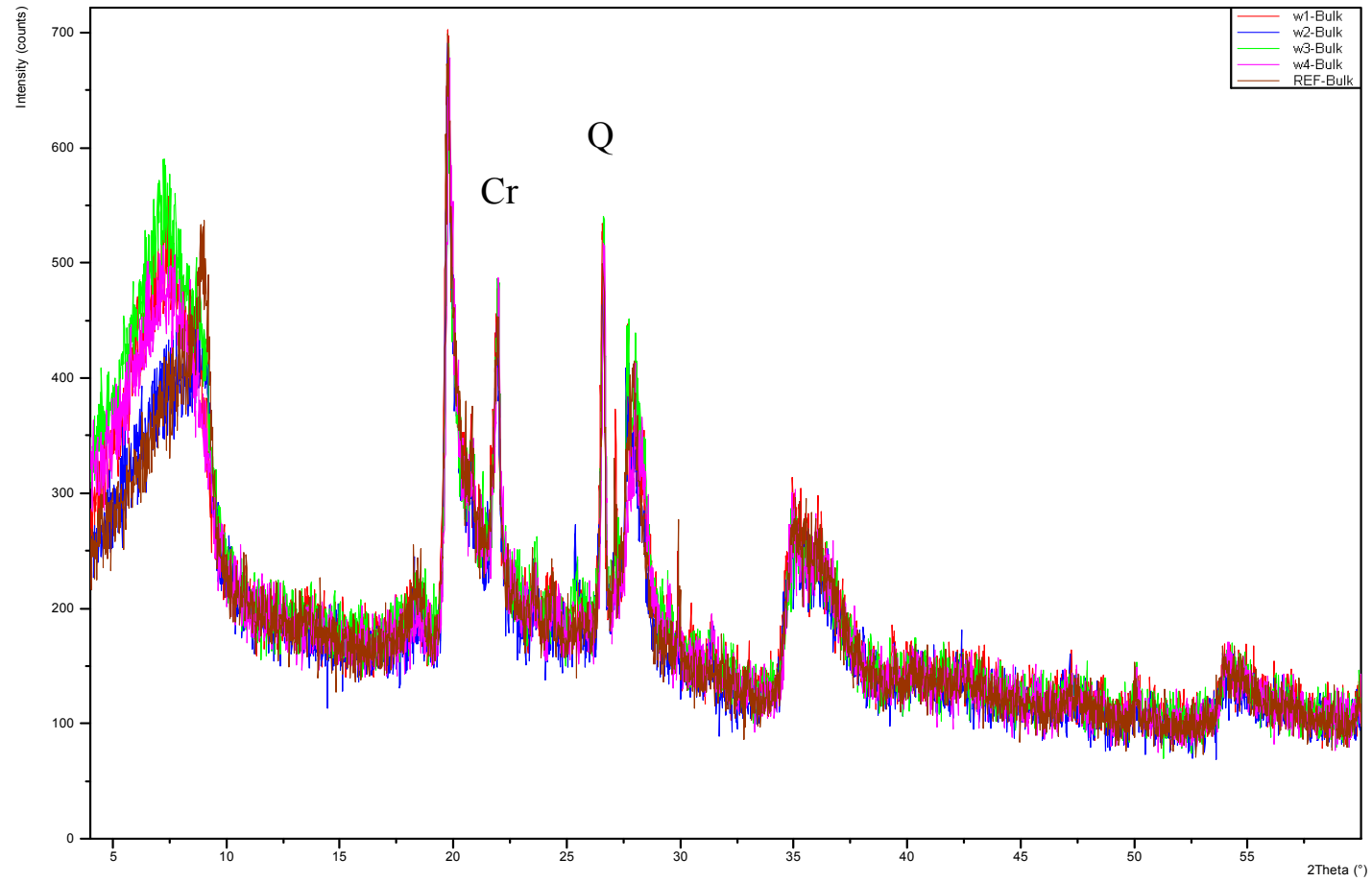


Figure 32: Disoriented bulk samples: Profile W1 to W4 compared to reference sample (REF-Bulk). Cr = cristobalite; Q = quartz

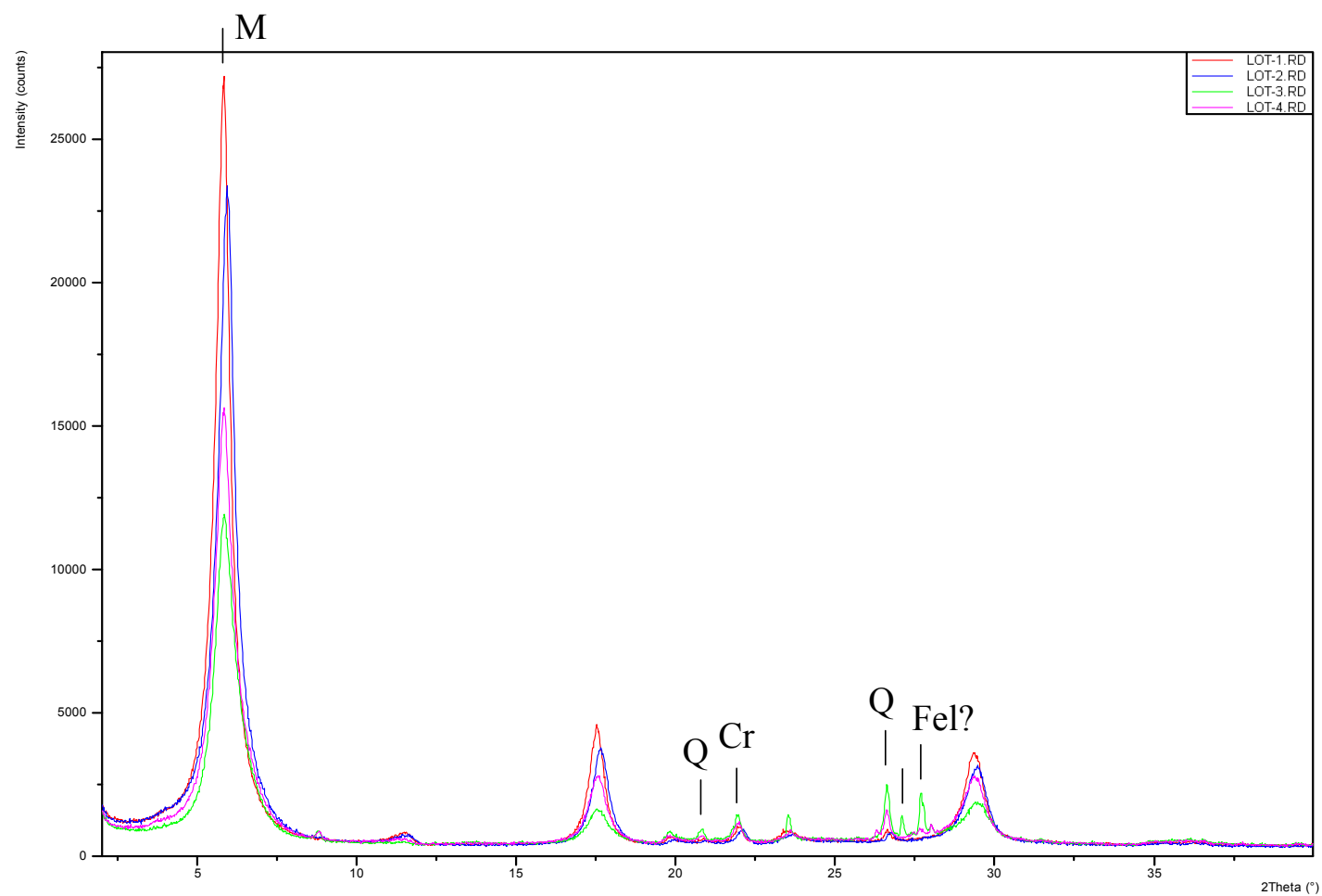


Figure 33: Test samples for optimizing measurement conditions. Cr = cristobalite; Q = quartz; Fel = feldspars; M = montmorillonite

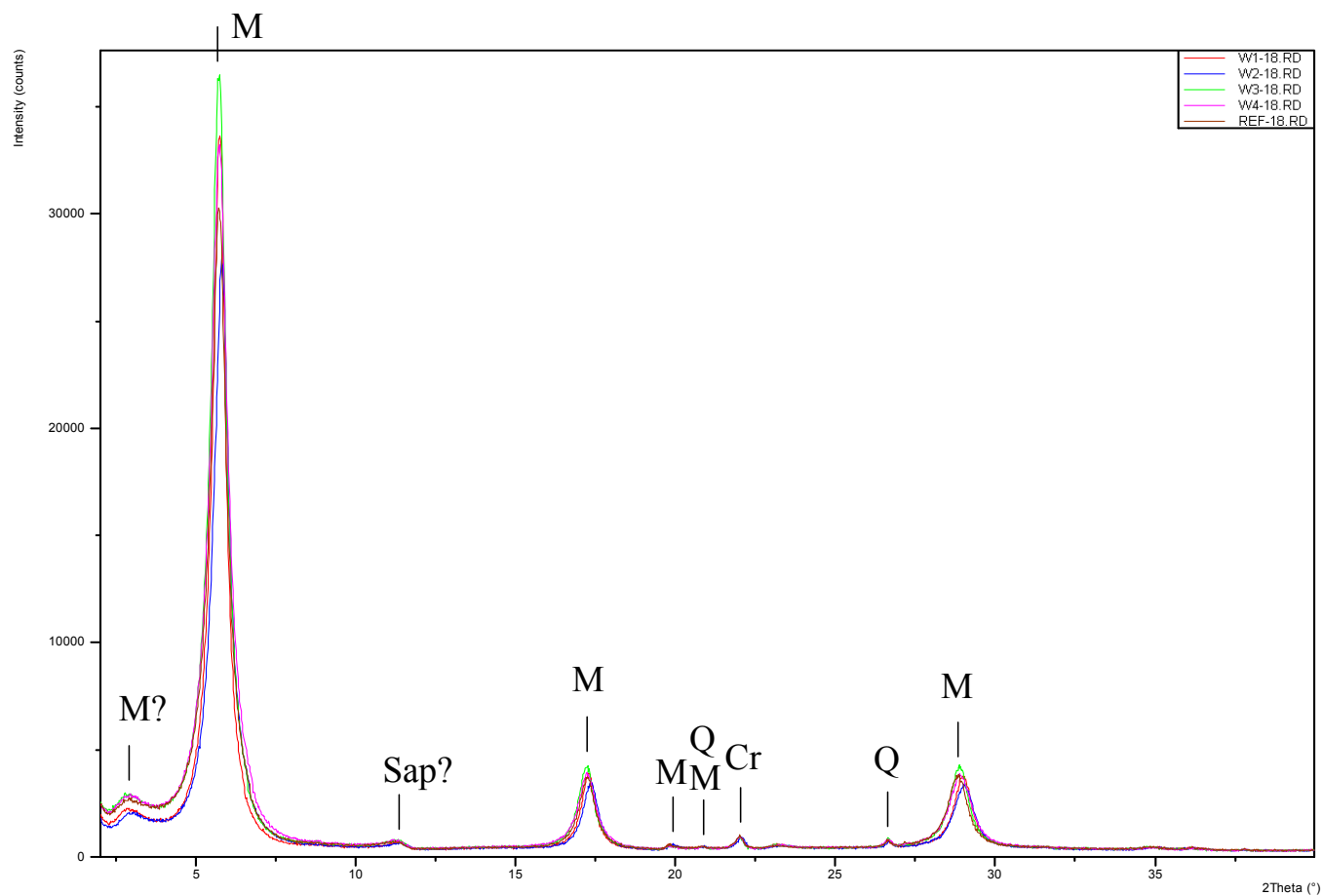


Figure 34: Oriented clay samples, 18 hours of sedimentation. Profile W1 to W4 compared to reference. Cr = cristobalite; Q = quartz; M = montmorillonite; Sap = saponite

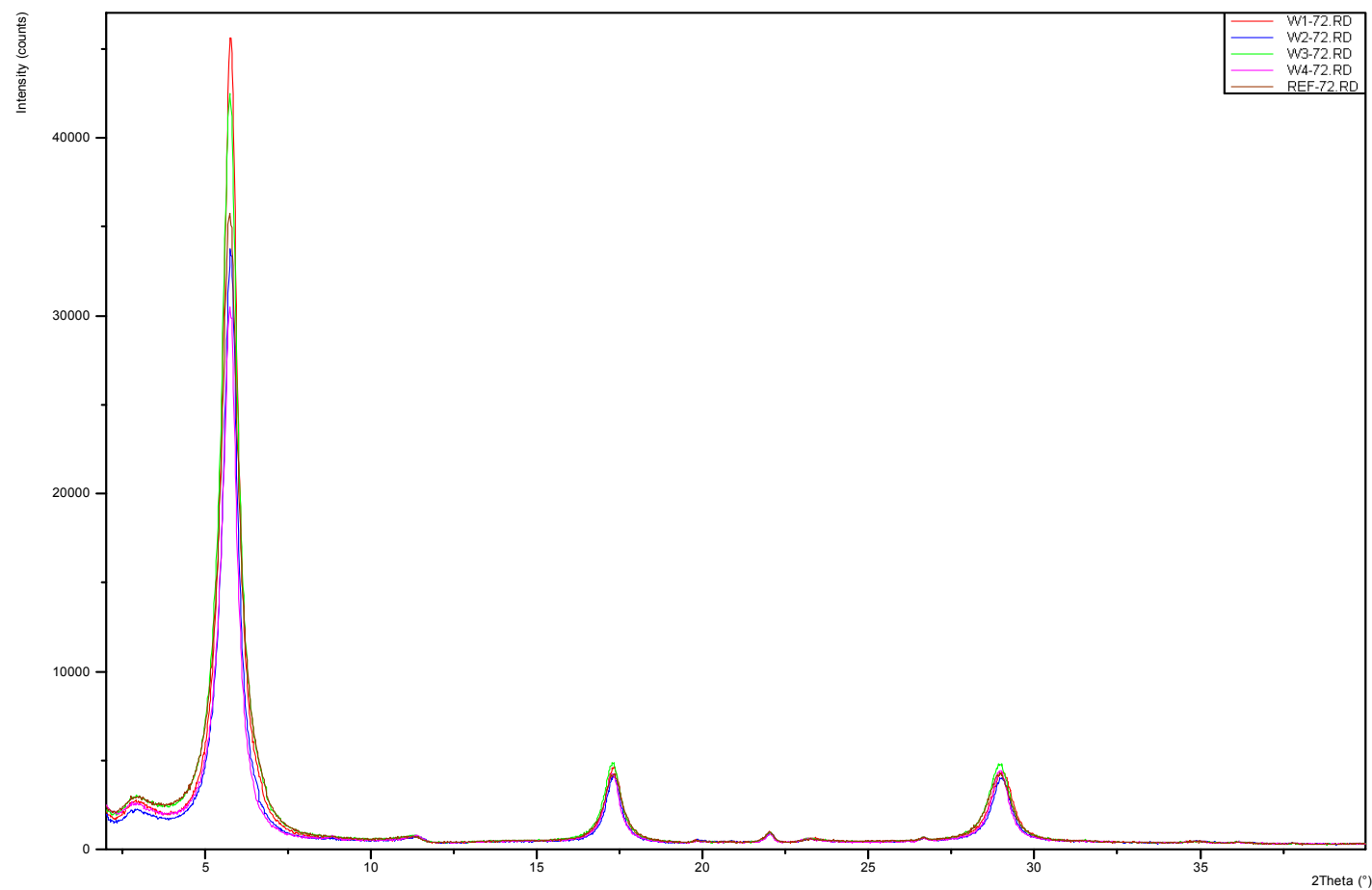


Figure 35: Oriented clay samples, 72 hours of sedimentation. Profile W1 to W4 compared to reference. See Figure 34 for peak labels

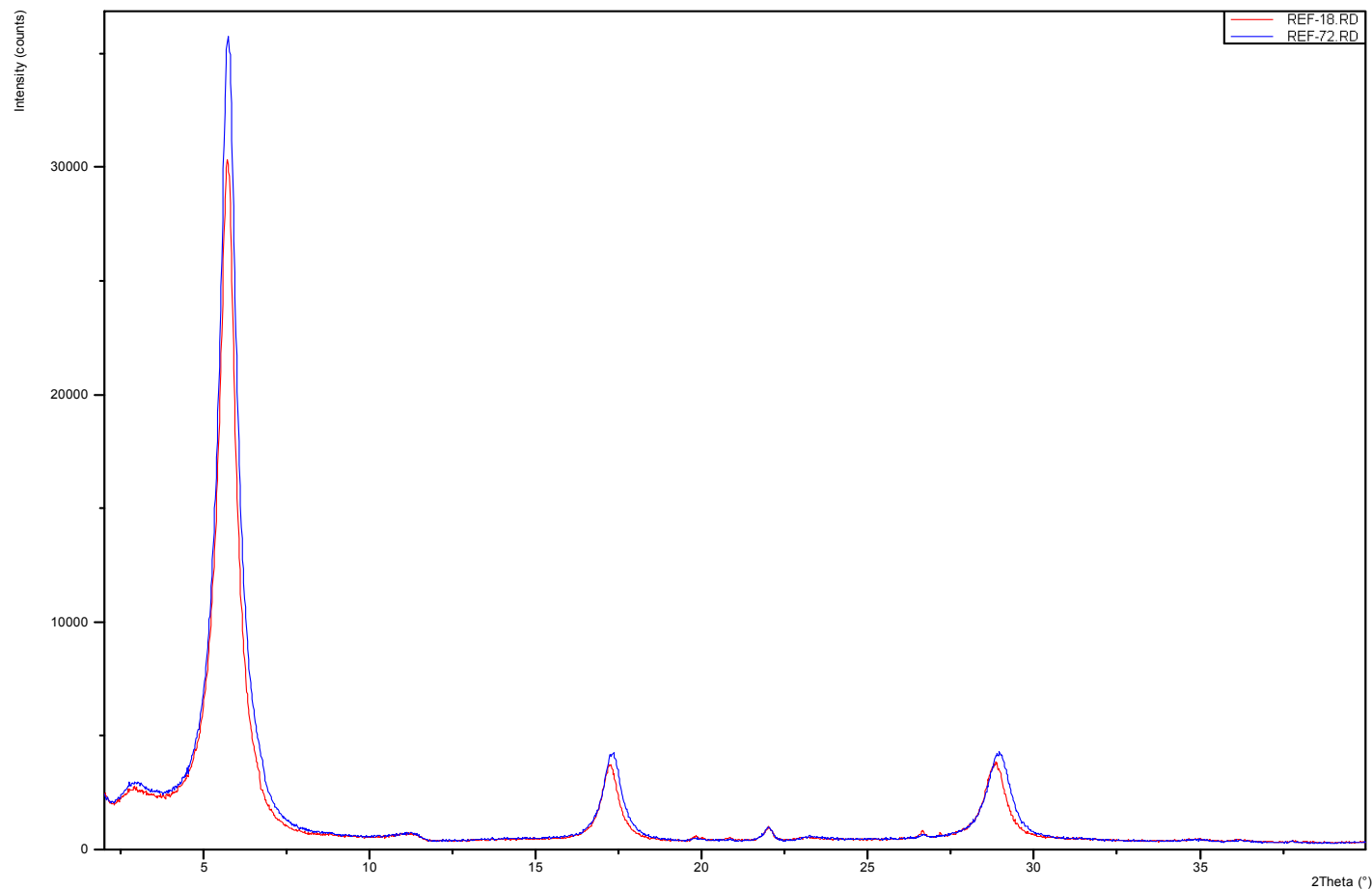


Figure 36: Comparison between 18 and 72 hours of sedimentation, reference sample. See Figure 34 for peak labels

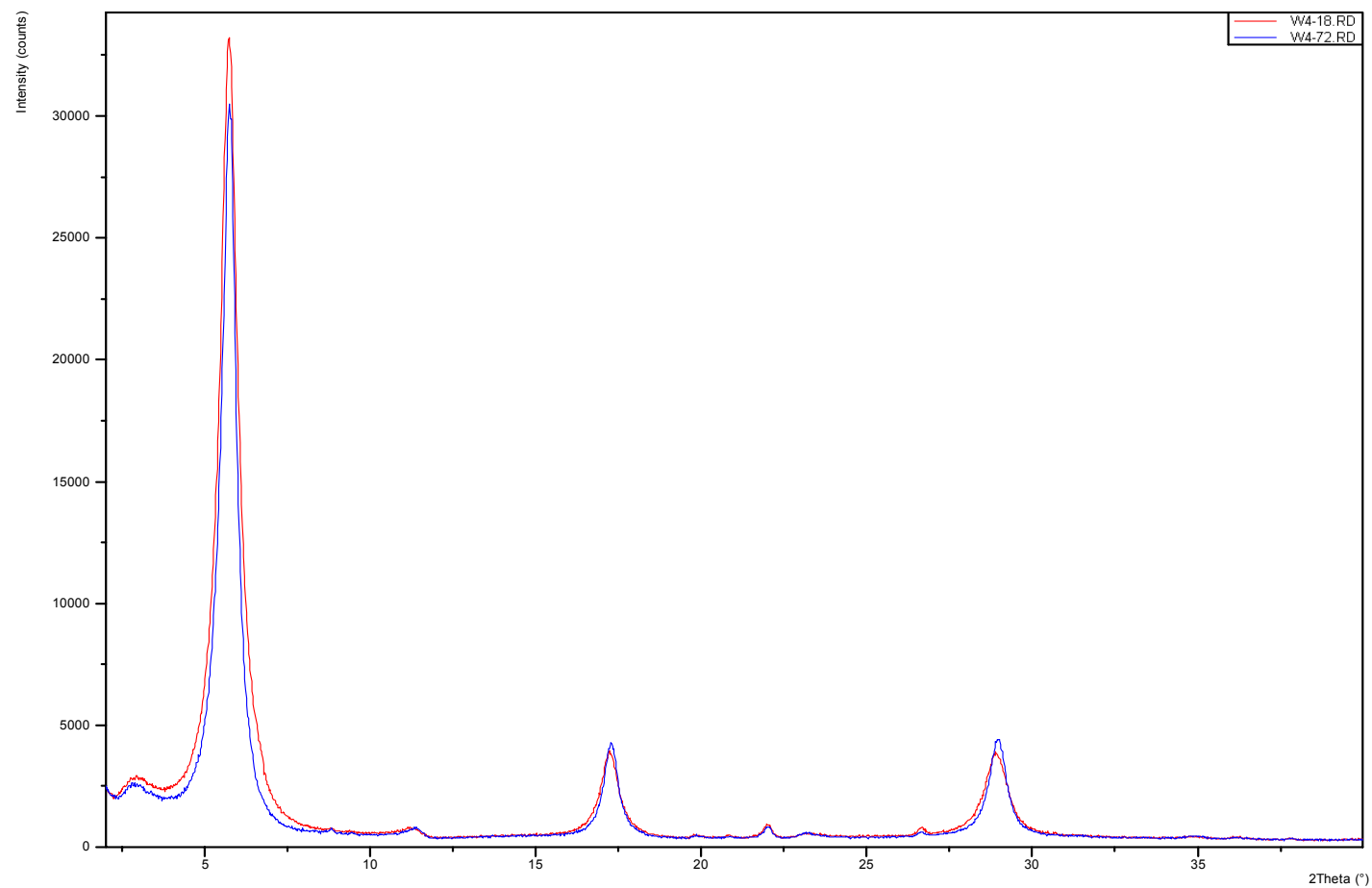


Figure 37: Comparison between 18 and 72 hours of sedimentation, profile sample W4 (cold end). See Figure 34 for peak labels

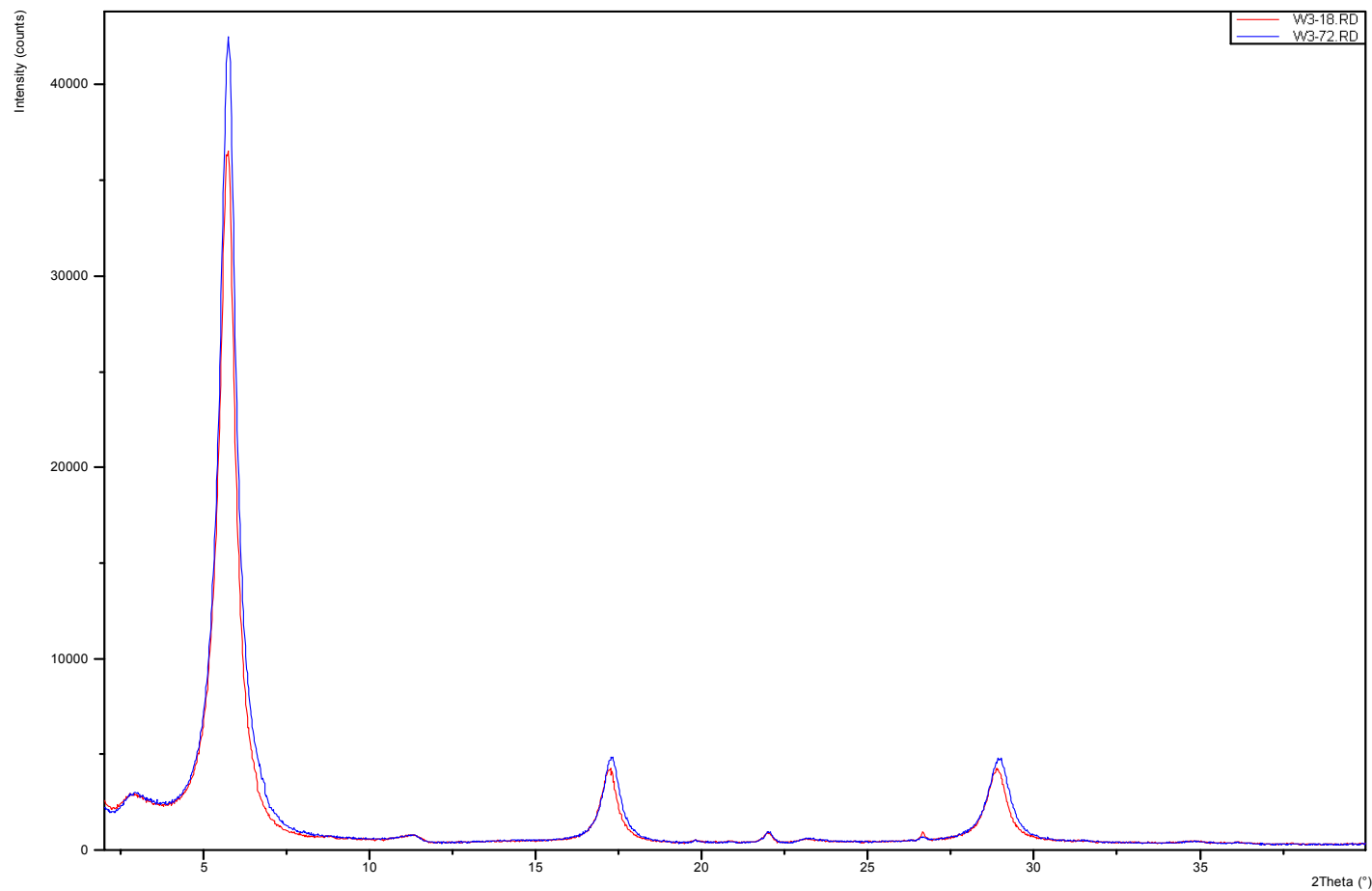


Figure 38: Comparison between 18 and 72 hours of sedimentation, profile sample W3. See Figure 34 for peak labels

B-15

NAGRA NAB 08-08

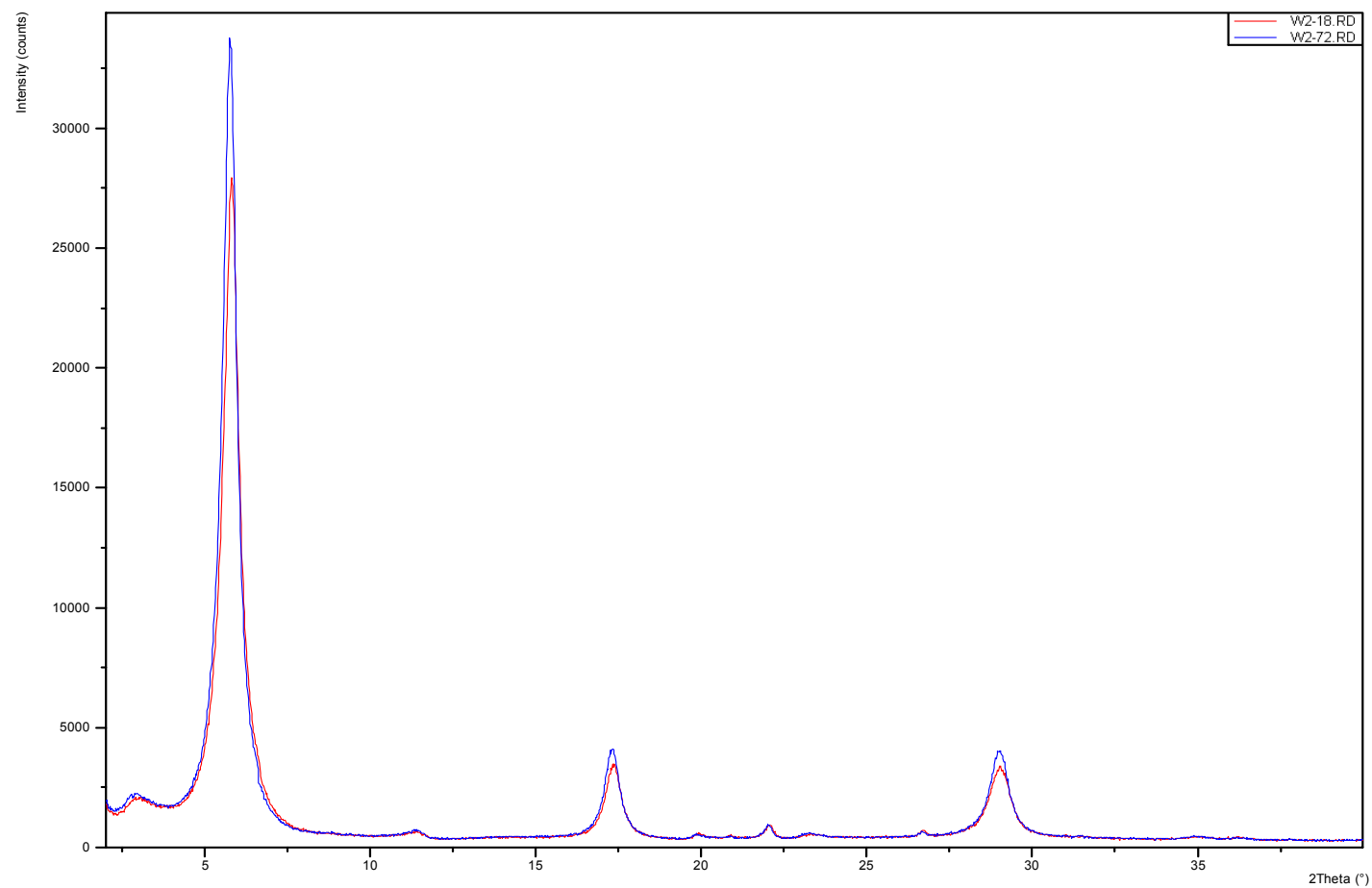


Figure 39: Comparison between 18 and 72 hours of sedimentation, profile sample W2. See Figure 34 for peak labels

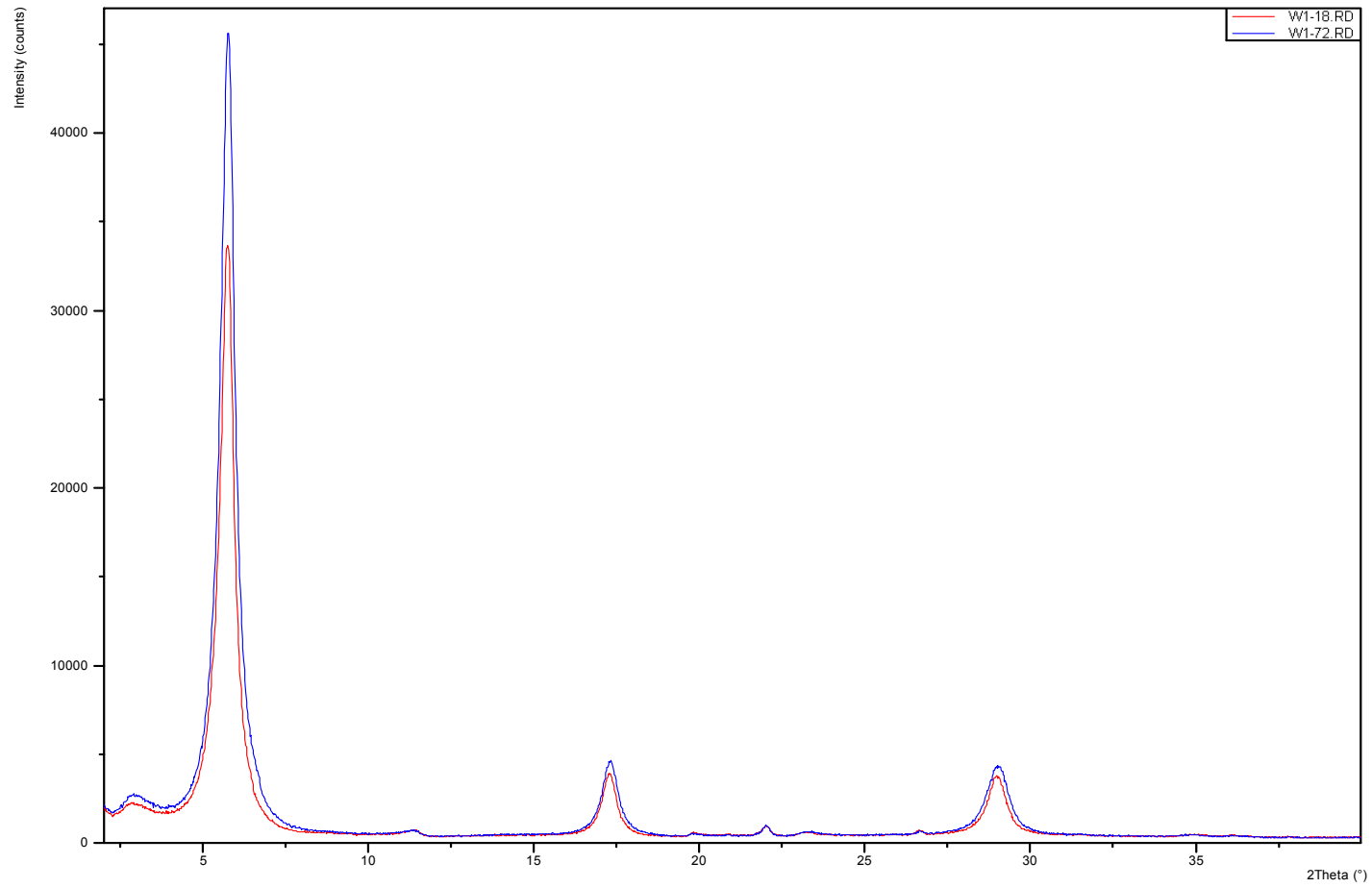


Figure 40: Comparison between 18 and 72 hours of sedimentation, profile sample W1 (hot end). See Figure 34 for peak labels

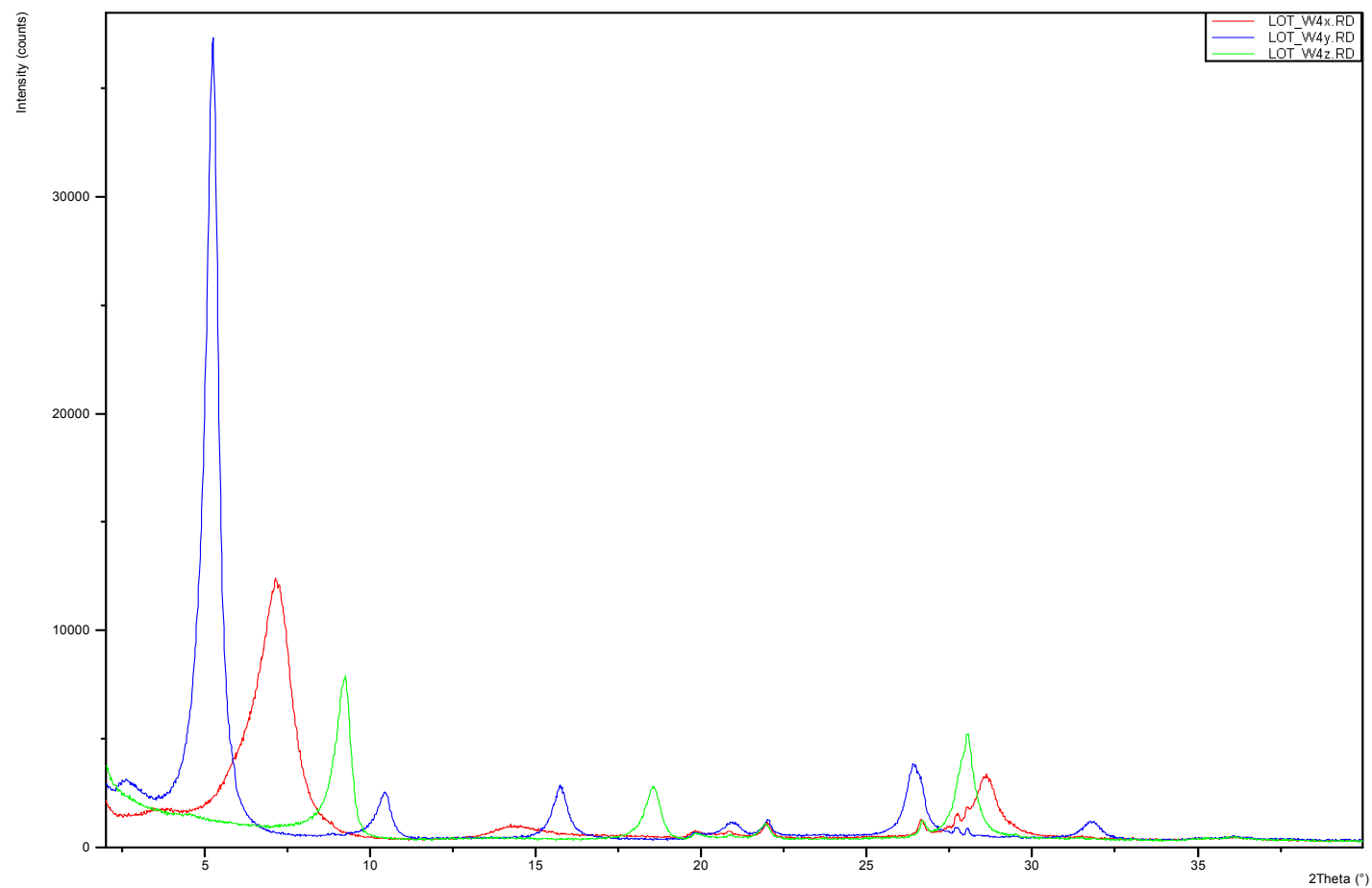


Figure 41: Profile sample W4 (cold end): x = dry sample; y = ethylenglicol saturated; z = heated at 550 °C for 2 h

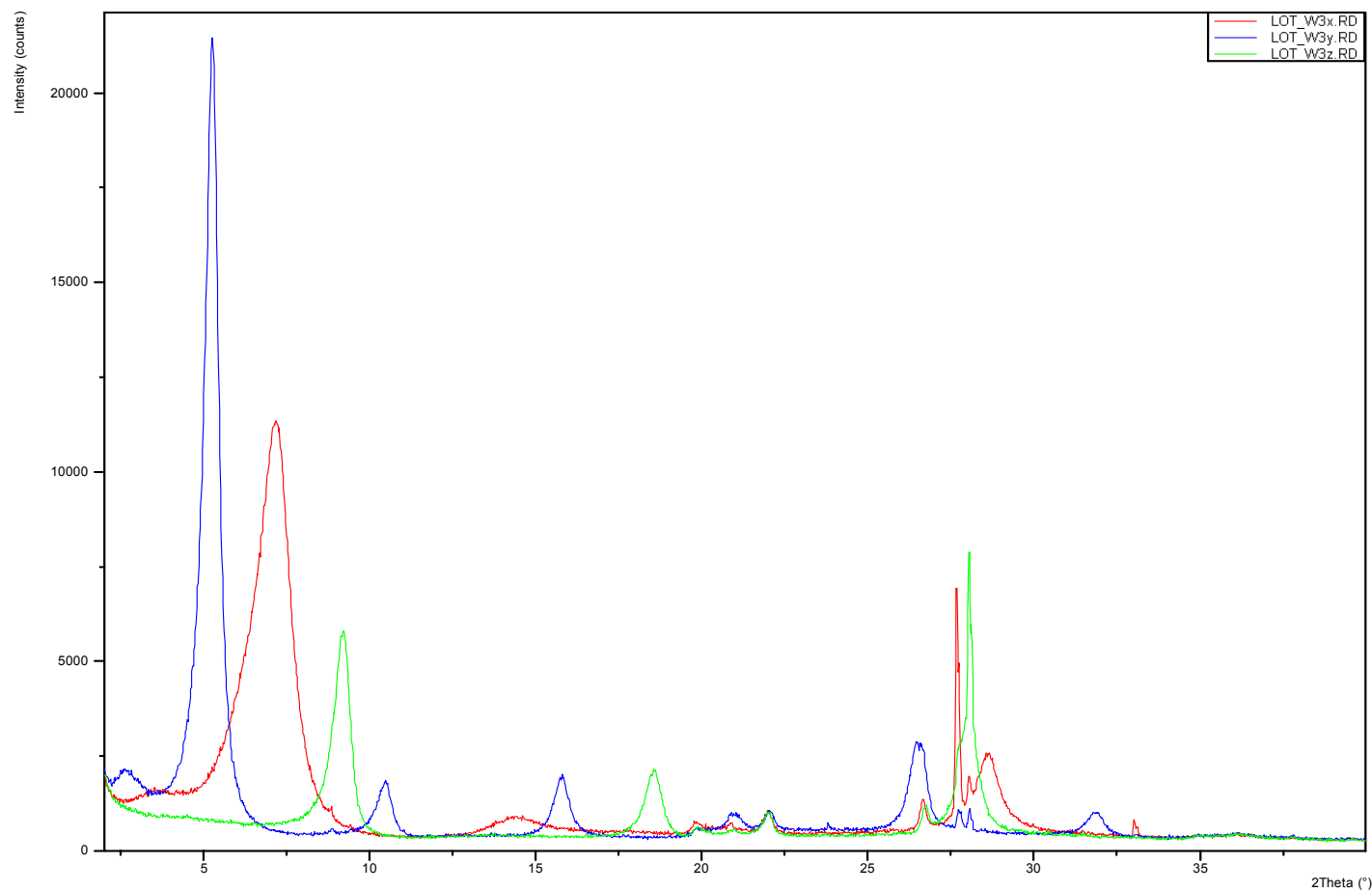


Figure 42: Profile sample W3: x = dry sample; y = ethylenglicol saturated; z = heated at 550 °C for 2 h

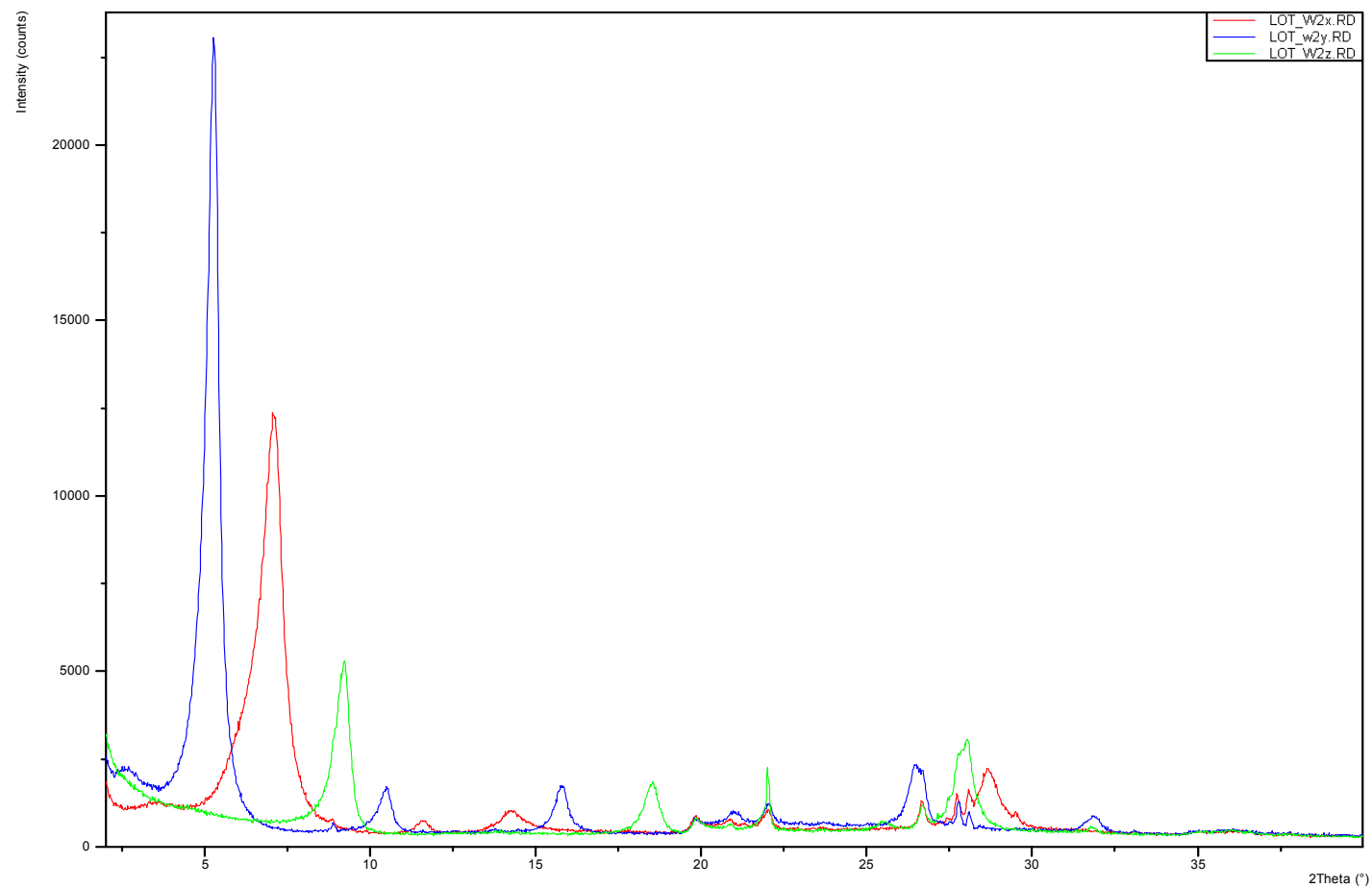


Figure 43: Profile sample W2: x = dry sample; y = ethylenglicol saturated; z = heated at 550 °C for 2 h

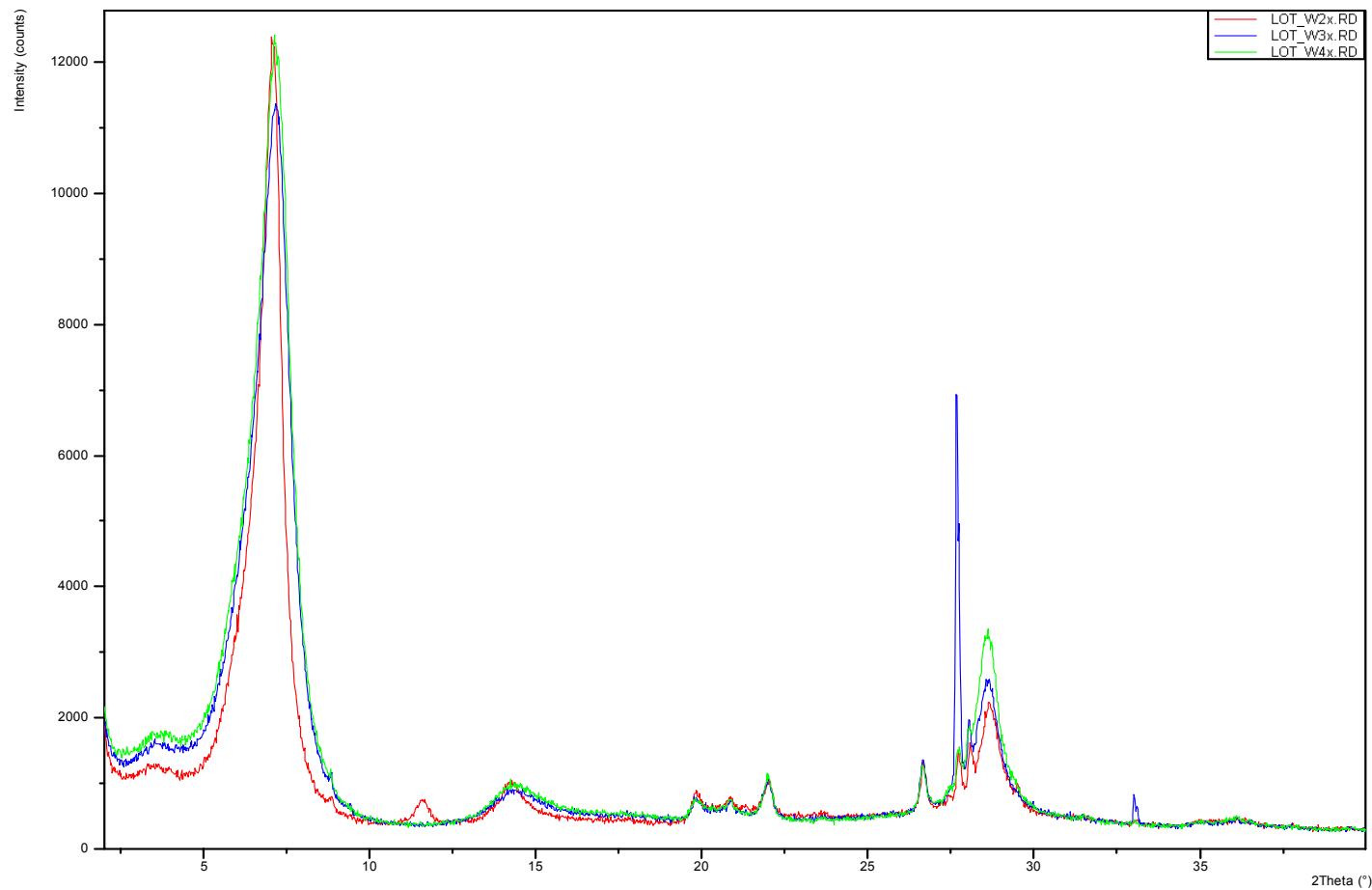


Figure 44: Profile sample W2, W3 and W4 (cold end): oriented dry samples

Appendix C - Aqueous extract data

Cation and anion concentrations of aqueous extracts from Block 13 of Parcel A2 of the LOT Experiment are summarized in Table 17.

Table 17: Aqueous extract concentrations in samples from LOT A2, Block 13 (mmol/l)

Sample (S:L = 0.1:1)	Na ⁺	K ⁺	Mg ⁺²	Ca ⁺²	Sr ⁺²	F ⁻	Cl ⁻	Br ⁻	SO ₄ ²⁻	NO ₃ ⁻	Alkalinity (as HCO ₃ ⁻)	pH	Charge balance error (%)
LOT A2-13 - 1	13.31	0.15	0.04	0.12	1.63E-03	0.06	0.40	6.50E-03	4.17	1.30E-01	4.40	9.19	1.60
LOT A2-13 - 2	13.28	0.13	0.02	0.11	1.68E-03	0.06	0.40	N.D.	4.20	1.30E-01	4.31	9.16	1.35
W-1B - 1	14.98	0.17	0.04	0.19	1.97E-03	0.05	2.69	6.53E-03	4.93	1.54E-02	2.60	8.73	1.22
W-1B - 2	15.69	0.19	0.05	0.18	2.00E-03	0.05	2.71	6.57E-03	5.30	1.70E-02	2.55	8.95	1.24
W-2B - 1	22.09	0.31	0.09	0.48	6.29E-03	0.04	2.74	N.D.	9.84	1.24E-02	1.65	8.91	1.26
W-2B - 2	22.03	0.31	0.08	0.47	6.36E-03	0.04	2.66	N.D.	9.78	1.25E-02	1.52	8.96	0.73
W-3B - 1	15.64	0.19	0.04	0.16	2.53E-03	0.06	3.14	N.D.	5.46	1.36E-02	2.14	9.18	0.15
W-3B - 2	14.86	0.18	0.03	0.14	2.73E-03	0.06	3.13	N.D.	4.94	1.35E-02	2.23	9.11	0.24
W-4B - 1	10.21	0.12	0.01	0.08	6.86E-04	0.10	3.78	6.52E-03	1.20	1.39E-02	3.41	9.30	4.05
W-4B - 2	10.28	0.10	0.02	0.08	6.93E-04	0.10	3.81	5.35E-03	1.16	1.31E-02	3.45	9.26	4.61

N.D. = not detected

Appendix D - Exchangeable cation data

Uncorrected cation concentrations derived from Ni-en extracts expressed in meq per 100 g dry mass from Block 13 of Parcel A2 of the LOT Experiment are summarized in Table 18. Also included is the sum of the cations and the total Ni consumption.

Table 18: Uncorrected concentrations of exchangeable cations recalculated to dry mass (meq/100 g) and total Ni consumption

Sample S:L	pH	Ca	Mg	K	Na	Sr	Cu	meq cat./100g	meq Ni/100g
Ni LOT A2-13 0.5/1	7.86	17.0	4.19	1.38	58.1	4.71e-1	N.D.	81.14	110.8
Ni LOT A2-13 0.5/2	7.87	17.5	4.09	1.36	58.1	4.67e-1	N.D.	81.52	111.0
Ni W-1B 0.5/1	8.25	25.0	6.06	1.30	55.4	4.51e-1	1.64	89.85	107.7
Ni W-1B 0.5/2	8.24	25.0	6.26	1.28	55.2	4.49e-1	1.63	89.82	107.1
Ni W-2B 0.5/1	8.14	27.7	5.14	1.54	59.1	5.08e-1	1.51e-2	94.00	115.1
Ni W-2B 0.5/2	8.13	27.3	5.12	1.54	59.3	5.20e-1	1.52e-2	93.80	116.2
Ni W-3B 0.5/1	8.09	23.0	4.97	1.37	59.0	4.92e-1	1.49e-3	88.83	115.0
Ni W-3B 0.5/2	8.08	22.8	5.09	1.36	59.1	4.84e-1	1.53e-3	88.84	115.7
Ni W-4B 0.5/1	8.05	16.2	5.47	1.29	60.6	4.50e-1	6.98e-2	84.08	113.3
Ni W-4B 0.5/2	8.05	16.2	5.33	1.25	59.7	4.46e-1	5.05e-2	82.98	114.8

N.D. = not detected